5-Substituted Imidazole-4-acetic Acid Analogues: Synthesis, Modeling, and Pharmacological Characterization of a Series of Novel γ-Aminobutyric Acid$_C$ Receptor Agonists

Christian Madsen,[†,#] Anders A. Jensen,[†,#] Tommy Liljefors,[†] Uffe Kristiansen,[‡] Birgitte Nielsen,[†] Camilla P. Hansen,[†] Mogens Larsen,[§] Bjarke Ebert,[§] Benny Bang-Andersen,[§] Povl Krogsgaard-Larsen,[†] and Bente Frølund*[,†]

Department of Medicinal Chemistry and Department of Pharmacology and Pharmacotherapy, Faculty of Pharmaceutical Sciences, University of Copenhagen, DK-2100 Copenhagen, Denmark, and Department of Medicinal Chemistry, H. Lundbeck A/S, DK-2500 Valby, Denmark

Received April 16, 2007

A series of ring-substituted analogues of imidazole-4-acetic acid (IAA, **4**), a partial agonist at both $GABA_A$ and $GABA_C$ receptors (GABA = γ-aminobutyric acid), have been synthesized. The synthesized compounds **8a**−**l** have been evaluated as ligands for the $\alpha_1\beta_2\gamma_{2S}$ $GABA_A$ receptors and the ρ_1 $GABA_C$ receptors using the FLIPR membrane potential (FMP) assay and by electrophysiology techniques. None of the tested compounds displayed activity at the $GABA_A$ receptors at concentrations up to 1000 μM. However, the 5-Me, 5-Ph, 5-*p*-Me-Ph, and 5-*p*-F-Ph IAA analogues, **8a**,**c**,**f**,**g**, displayed full agonist activities at the ρ_1 receptors in the FMP assay (EC_{50} in the range 22−420 μM). Ligand−protein docking identified the Thr129 in the α_1 subunit and the corresponding Ser168 residue in ρ_1 as determinants of the selectivity displayed by the 5-substituted IAA analogues. The fact that GABA, **4**, and **8a** displayed decreased agonist potencies at a ρ_1Ser168Thr mutant compared to the WT ρ_1 receptor strongly supported this hypothesis. However, in contrast to GABA and **4**, which exhibited increased agonist potencies at a α_1(Thr129Ser)$\beta_2\gamma_2$ mutant compared to WT $GABA_A$ receptor, the data obtained for **8a** at the WT and mutant receptors were nonconclusive.

Introduction

γ-Aminobutyric acid (GABA, Figure 1) is the major inhibitory neurotransmitter in the mammalian central nervous system (CNS), where it exerts its physiological effects through the ionotropic $GABA_A$ and $GABA_C$ receptors and the metabotropic $GABA_B$ receptors. The ionotropic GABA receptors belong to a superfamily of ligand-gated ion channels that also includes the nicotinic acetylcholine, the glycine, and the serotonin (5-HT_3) receptors.[1] Whether the $GABA_C$ receptor is a subgroup of the $GABA_A$ receptors or a distinct group of GABA receptors is still a matter of debate.[2,3] The $GABA_A$ receptors are widely distributed in the CNS and involved in a wide variety of CNS functions, whereas the $GABA_C$ receptors predominantly are expressed in the retina and primarily implicated in visual processing.[4,5] However, $GABA_C$ receptors have also been identified in some CNS regions, where they have been proposed to be involved in processes connected to regulation of sleep and cognition processes.[6,7]

The ionotropic GABA receptors are transmembrane protein complexes composed of five subunits. So far, 19 human GABA receptor subunits have been identified, and they have been classified into α (α_1−α_6), β (β_1−β_3), γ (γ_1−γ_3), δ, ϵ, π, θ, and ρ (ρ_1−ρ_3) subunit classes. Each of the subunits consists of an amino-terminal domain and a transmembrane region consisting of four transmembrane α-helices connected by intra- and extracellular loops. In the pentameric GABA receptor complex the orthosteric site (i.e., the binding site for the endogenous agonist GABA) is formed at the interface between the amino-terminal domains of two subunits, whereas the transmembrane regions of the subunits form the ion channel pore through which Cl^- ions can enter the cell upon activation of the receptor. The $GABA_A$ receptors are heteromeric complexes, and although a wide range of different $GABA_A$ receptor combinations exist in vivo, the $\alpha_1\beta_2\gamma_2$ combination is the predominant physiological $GABA_A$ receptor subtype.[8,9] In contrast, the $GABA_C$ receptors are homomeric assemblies of five identical ρ subunits or

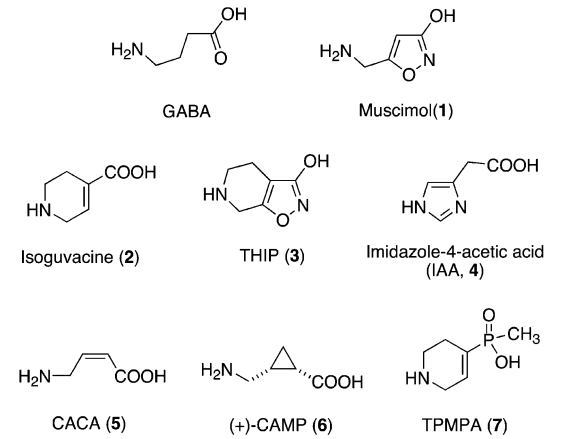

Figure 1. Structures of GABA, the $GABA_A$ agonists muscimol (**1**), isoguvacine (**2**), THIP (**3**), the partial $GABA_A$ and $GABA_C$ agonist IAA (**4**), the $GABA_C$ agonists CACA (**5**) and (+)-CAMP (**6**), the $GABA_C$ antagonist TPMPA (**7**), and the synthesized 2-, 5-, and 2,5-substituted IAA analogues (**8a**−**l**).

* To whom correspondence should be addressed. Phone: Phone: (+45) 3530649. Fax: (+45) 35306040. E-mail: bfr@farma.ku.dk.
† Department of Medicinal Chemistry, University of Copenhagen.
# C.M. and A.A.J. are co-first-authors.
‡ Department of Pharmacology and Pharmacotherapy, University of Copenhagen.
§ H. Lundbeck A/S.

10.1021/jm070447j CCC: $37.00
Published on Web 07/26/2007

pseudoheteromeric complexes comprising different ρ subunits.[10,11] Although recent studies have indicated that $GABA_A$ and $GABA_C$ receptor subunits are capable of forming heteromeric complexes in the CNS, the functional characteristics and physiological importance of these receptors have not been explored.[12]

The overall molecular architecture of the orthosteric sites of the $GABA_A$ and the $GABA_C$ receptors appear to be quite similar, as most $GABA_A$ agonists display some agonist/antagonist activities at $GABA_C$ receptors as well.[6] 4,5,6,7-Tetrahydroisoxazolol[5,4-*c*]pyridin-3-ol (THIP, **3**), a standard $GABA_A$ agonist, has been shown to be a partial agonist at $GABA_A$ receptors and a competitive antagonist at $GABA_C$ receptors.[13−15] Likewise, the $GABA_A$ agonists muscimol (**1**), isoguvacine (IGU, **2**), and imidazole-4-acetic acid (IAA,[a] **4**) act as partial $GABA_C$ receptor agonists.[15,16] However, the fact that $GABA_A$ and $GABA_C$ receptors exhibit distinct antagonist profiles clearly indicates that orthosteric sites of these receptors are not identical.[17]

The understanding of molecular architecture of the orthosteric sites in $GABA_A$ and $GABA_C$ receptors has been greatly increased by the publication of crystal structures of acetylcholine binding proteins (AChBPs) from snails.[18−20] These proteins display weak but significant amino acid sequence homologies with the amino-terminal domains of all ligand-gated ion channels, including the GABA receptors, and this homology has been exploited for the construction of homology models of this region in both $GABA_A$ and $GABA_C$ receptors.[21−23] Such homology models offer an insight into the identities of the residues lining the binding pockets in the respective receptors.

The relationship between the ligand structure and binding/activity at the $GABA_A$ receptor has been extensively studied.[24] On the basis of a hypothesis originating from the bioactive conformation of muscimol and on pharmacological data for a series of $GABA_A$ ligands, a 3D pharmacophore model for orthosteric $GABA_A$ receptor ligands has been developed.[25] In contrast, structure−activity studies of ligands targeting the $GABA_C$ receptor have been considerably more sparse.[15,26−28] *cis*-4-Aminocrotonic acid (CACA, **5**) has been the key ligand for the identification of the $GABA_C$ receptors.[29] The compound is a moderately potent partial $GABA_C$ agonist and inactive at $GABA_A$ receptors, but it has been shown to effect GABA transport as well.[15,30] In the search for selective $GABA_C$ receptor ligands, the folded conformation of CACA has been used as a scaffold for new compounds such as *cis*-2-aminomethylcyclopropanecarboxylic acid (CAMP). (+)-CAMP (**6**) has been reported to be a selective $GABA_C$ receptor agonist with a potency in the mid-micromolar range, displaying only weak activity at the $GABA_A$ receptors and having no effects on GABA transport.[31] Finally, the first antagonist capable of differentiating the $GABA_C$ receptors from both $GABA_A$ and $GABA_B$ receptors was (1,2,5,6-tetrahydropyridin-4-yl)methylphosphinic acid (TPMPA, **7**).[17,32]

In the present study, we report the design, synthesis, and pharmacological characterization of a series of ring substituted analogues of IAA (**4**, Figure 1), a partial agonist at both $GABA_A$ and $GABA_C$ receptors. Furthermore, the molecular basis for the pharmacological characteristics of some of these compounds has been investigated in a mutagenesis study based on homology models of the $GABA_A$ and $GABA_C$ receptor amino-terminal domains.

Scheme 1[a]

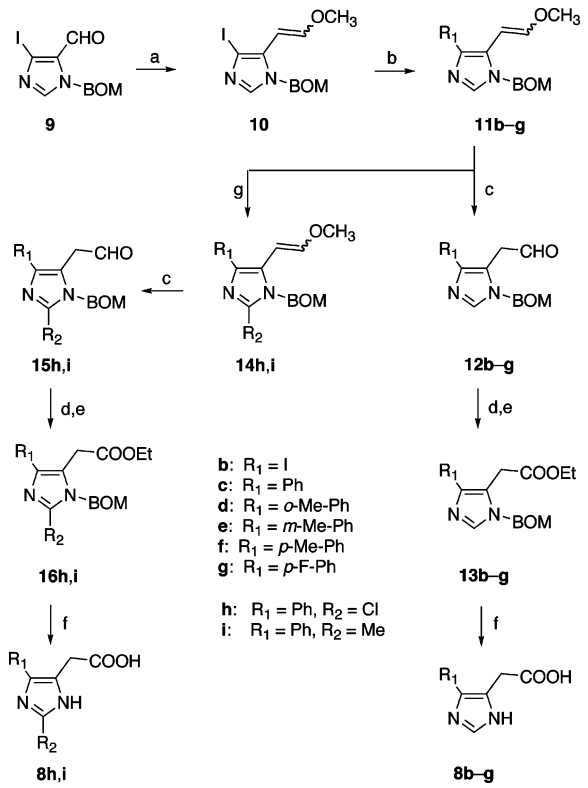

[a] Reagents: (a) $CH_3OCH_2P^+Ph_3Cl^-$, NaHMDS, THF, 0 °C to room temp; (b) $RB(OH)_2$, K_3PO_4(aq), $Pd(PPh_3)_2Cl_2$, 1,4-dioxane, 110 °C; (c) 6 M HCl(aq), 1,4-dioxane, 70 °C; (d) $NaClO_2$(aq), $NaH_2PO_4 \cdot H_2O$, 2-methyl-2-butene in CH_3CN, room temp, then 6 M HCl(aq); (e) HCl/EtOH; (f) 48% HBr(aq), 110 °C; (g) *n*-BuLi, C_2Cl_6 or CH_3I, THF, −78 °C.

Results

Chemistry. The synthesis of the 5(4)-aryl substituted IAA analogues is illustrated in Scheme 1. The key intermediate in this strategy was the enol ether **10**, which was synthesized from **9** using a Wittig reaction. The preparation of **9** in three steps from imidazole has previously been published,[33] and modifications of these procedures were used. Suzuki cross-coupling between **10** and appropiate arylboronic acids provided **11b**−**g**, which as well as **10** were converted to the corresponding aldehydes **12b**−**g** in high yields. The subsequent $NaClO_2$ oxidation to the corresponding carboxylic acids proceeded smoothly; however, because of purification problems, the acids were subjected to Fischer esterification to yield **13b**−**g**, which could be purified by column chromatography. Deprotection using aqueous HBr gave the IAA analogues **8b**−**g**. Further introduction of substituents in the 2-postion was accomplished by treatment of **11c** with *n*-BuLi followed by C_2Cl_6 or CH_3I as electrophiles giving **14h** and **14i**, respectively, which were converted to **8h** and **8i** by use of the same synthetic procedures as described for **8b**−**g**.

Attempts to use the same strategy for the synthesis of IAA analogues with substituents smaller than aryl or iodine failed. Numerous attempts to hydrolyze the resulting enol ether all resulted in severe polymerization of the corresponding aldehyde.

Instead, the 5(4)-methyl IAA analogue (**8a**) was prepared from commercially available 4(5)-hydroxymethyl-5(4)-methylimidazole (**19a**, Scheme 2). Conversion to the cyano com-

[a] Abbreviations: IAA, imidazole-4-acetic acid; THIP, tetrahydroisoxazolol[5,4-*c*]pyridin-3-ol; CACA, *cis*-4-aminocrotonic acid; CAMP, *cis*-2-aminomethylcyclopropanecarboxylic acid; TPMPA, (1,2,5,6-tetrahydropyridin-4-yl)methylphosphinic acid; IGU, isoguvacine; FLIPR, fluorescent imaging plate reader; FMP, FLIPR membrane potential; DCVC, dry vacuum chromatography.

Scheme 2[a]

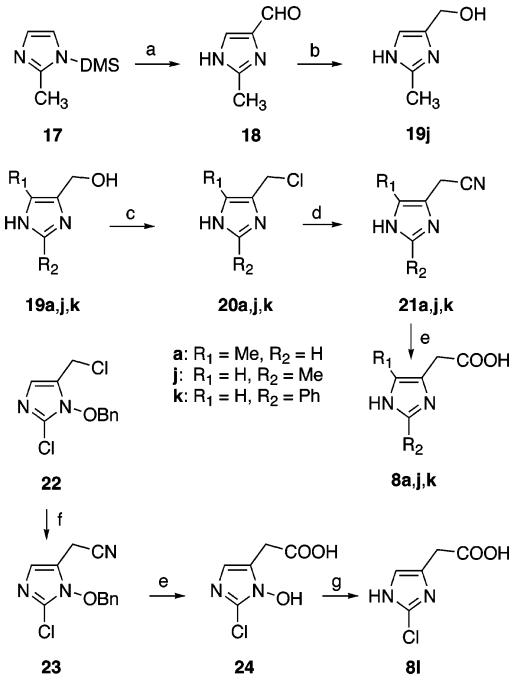

[a] Reagents: (a) *n*-BuLi, THF, then DMF, −78 °C; (b) $NaBH_4$, EtOH; (c) $SOCl_2$, room temp or 80 °C; (d) NaCN, DMSO, room temp; (e) 48% HBr(aq), 110 °C, then HCl/EtOH, reflux; (f) KCN, DMF, H_2O, room temp; (g) 10% $TiCl_3$ in 20% HCl(aq), MeOH, 0 °C.

pound **21a** via the chloride **20a** was performed as described by Rosen et al.[34] Hydrolysis of the cyano group was undertaken by use of aqueous HBr to afford **8a**. The 2-methyl analogue (**8j**) was prepared using the dimethylsulfamoyl protected 2-methylimidazole (**17**)[35] as starting compound. Treatment with *n*-BuLi followed by DMF and acidic aqueous workup afforded the corresponding deprotected aldehyde (**18**), which after $NaBH_4$ reduction resulted in the hydroxymethyl analogue **19j**. The corresponding 4(5)-hydroxymethyl-2-phenyl (**19k**) was synthesized according to the literature procedure in which benzamidine and dihydroxyacetone are condensed in aqueous ammonia at 80 °C.[36] The overall strategy used in the synthesis of **8a** was then used to convert the two hydroxymethyl analogues to the desired IAA analogues (**8j**,**k**).[36,37] However, as in the synthesis of the 5(4)-aryl substituted analogues the final compounds were obtained via the esters. The 2-chloro analogue (**8l**) was prepared from **22**,[38] which was converted to **24** by use of the same strategy used in the synthesis of **8a**. Removal of the *N*-hydroxy group was undertaken with $TiCl_3$ to provide **8l**.

In Vitro Pharmacology. Since IAA (**4**) is a standard agonist at both $GABA_A$ and $GABA_C$ receptors, the pharmacological properties of the synthesized 2- and 5-substituted IAA analogues, **8a**−**l**, were characterized at both these receptor classes. The binding affinities of the compounds at native $GABA_A$ receptors (predominantly $\alpha_1\beta_2\gamma_{2S}$ $GABA_A$ receptors) were determined in a [^{3}H]muscimol binding assay using rat brain membrane preparations, and the functional properties of selected analogues were determined at human $\alpha_1\beta_2\gamma_{2S}$ $GABA_A$ receptors expressed in *Xenopus* oocytes using two-electrode voltage-clamp electrophysiology. As seen from Table 1, only the 5-methyl substituted analogue **8a** exhibited measurable affinity for the native $GABA_A$ receptors, and its binding affinity was 100-fold lower than that displayed by the parent compound **4**. None of the tested compounds **8a**−**l** displayed any measurable activity at the human $\alpha_1\beta_2\gamma_{2S}$ $GABA_A$ receptor subtype at concentrations up to 1000 μM (Table 1).

The functional properties of the IAA analogues at the $GABA_C$ receptor were characterized in the FLIPR membrane potential (FMP) assay using a stable HEK293 cell line expressing the human homomeric ρ_1 receptor. The 2-substituted IAA analogues, **8h**−**k**, were inactive both as agonists and as antagonists at the ρ_1-HEK293 cell line at concentrations up to 1000 μM (Table 1). In contrast, the 5-methyl analogue **8a** displayed an agonist potency similar to that of **4** at the receptor. Introduction of a phenyl ring in the 5-position was also tolerated, although compound **8c** exhibited a 32-fold lower agonist potency than **4**. Introduction of a methyl group or a fluoro atom in the para position of the phenyl ring (compounds **8f** and **8g**) resulted in slightly increased agonist potencies compared to that of compound **8c**. On the other hand, methyl substitutions into the ortho or meta positions of the phenyl ring, yielding compounds **8d** and **8e**, respectively, were detrimental to the ρ_1 receptor activity, as both compounds were inactive at concentrations up to 1000 μM (Table 1). Introduction of an iodo atom directly in the 5-position of **4** also eliminated activity at the ρ_1 receptor (compound **8b**).

Interestingly, the maximal responses displayed by the 5-substituted IAA analogues at the ρ_1 receptor in the FMP assay increased with the size of the 5-substituent. **4** was a clear-cut partial agonist exhibiting a maximal response of 32% relative to the maximal response of GABA at the receptor, whereas the 5-methyl and 5-phenyl analogues (compounds **8a** and **8c**) were full agonists at the receptor (Table 1 and Figure 2). Finally, compounds **8f** and **8g** displayed tendencies toward superagonism with maximal responses of 111% and 115%, respectively (Table 1 and Figure 2).

$GABA_A$ and $GABA_C$ Ligand−Receptor Modeling. In order to identify structural determinants for the observed selectivity for ρ_1GABA_C over $\alpha_1\beta_2\gamma_2GABA_A$ receptors displayed by the 5-substituted IAA analogues **8a**, **8c**, **8f**, and **8g**, homology models based on the model of the amino-terminal domain of the $\alpha_1\beta_2\gamma_2GABA_A$ receptor developed by Ernst et al. were employed.[21] This model was developed by comparative modeling based on the X-ray crystal structure of the *Lymnae stagnalis* acetylcholine binding protein (AChBP).[20]

As mentioned above, a high degree of similarity exists between the orthosteric binding pockets in the $GABA_A$ and $GABA_C$ receptors. Of the 13 residues in the residue interval 100−250 in the ρ_1 $GABA_C$ receptor pointing toward the putative agonist binding site and identified by mutational studies as being key binding site residues,[22] 10 residues are either identical or conservatively substituted (Tyr/Phe, Thr/Ser, and Val/Leu) in the $GABA_A$ $\alpha_1\beta_2$ interface. These 10 highly conserved residues have also been identified as key binding site residues in the $GABA_A$ receptor.[22] For the purpose of the present study, these strong similarities indicate that the $GABA_A$ and $GABA_C$ binding pockets are sufficiently similar to allow us to use the $GABA_A$ receptor model and substitute divergent residues with respect to the ρ_1 $GABA_C$ receptor to provide a model for the $GABA_C$ binding pocket. The high similarity of the two binding pockets also indicates that GABA and other agonists bind in a similar way in the two receptors.

GABA, IAA (**4**), and the 2- and 5-substitued IAA analogues **8a**−**l** were manually docked into the $GABA_A$ $\alpha_1\beta_2$ interface on the basis of the mutational studies referred to above and using the bioactive conformations of the ligands deduced from our previously reported pharmacophore model.[25,39,40] The ligands were docked into the orthosteric site of the ρ_1 $GABA_C$ receptor in the same orientation as in the $GABA_A$ receptor. The resulting ligand orientations and receptor interactions are shown in Figure

Table 1. $GABA_A$ Receptor Binding Affinities at Rat Synaptic Membranes and Functional Data on Oocytes Expressing $\alpha_1\beta_2\gamma_{2S}$ Receptors Using Two-Electrode Voltage-Clamp and on hρ_1-HEK293 Cell Line in FMP Assay[a]

		$\alpha_1\beta_2\gamma_{2S}$ expressed in *Xenopus* oocytes		ρ_1-HEK293 cell line	
	[^{3}H]muscimol binding K_i (μM)[b] [pK_i ± SEM]	EC_{50} (μM)[b] [pEC_{50} ± SEM]	R_{max}	EC_{50} (μM)[b] [pEC_{50} ± SEM]	R_{max} ± SEM
GABA	0.018[c]	80[d]	100[d]	0.55 [6.3 ± 0.03]	100
muscimol (**1**)	0.006[e]	4[f]	100[f]	2.2 [5.7 ± 0.05]	101 ± 5
IGU (**2**)	0.22[c]	160[d]	88[d]	67 [4.2 ± 0.03]	97 ± 3
THIP (**3**)	0.092[c]	238[g]	70[g]	100 [4.0 ± 0.06][h]	
IAA (**4**)	0.65 [6.2 ± 0.01]	310[d]	24[d]	13 [4.9 ± 0.05]	32 ± 5
CACA (**5**)	nd	>5000[i]		37.4[j]	75[j]
(+)-CAMP (**6**)	nd	>1000[k]		39.7[k]	104[k]
TPMPA (**7**)	39[l]	320 (K_b)[m]		1.3 [5.9 ± 0.04][h]	
8a	67 [4.2 ± 0.03]	>1000		22 [4.6 ± 0.04]	95 ± 6
8b	>100	nd		>1000	
8c	>100	>1000		420 [3.4 ± 0.04]	98 ± 3
8d	>100	nd		>1000	
8e	>100	nd		>1000	
8f	>100	nd		240 [3.6 ± 0.05]	111 ± 3
8g	>100	nd		210 [3.7 ± 0.04]	115 ± 6
8h	>100	nd		>1000	
8i	>100	>1000		>1000	
8j	>100	nd		>1000	
8k	>100	nd		>1000	
8l	>100	>1000		nd	

[a] The R_{max} values are % of the maximal response of GABA. The data are based on at least three experiments performed in dublicate. nd, not determined. [b] K_i and EC_{50} values were calculated from pK_i and pEC_{50} values found in brackets. [c] Data from Frølund et al.[72] [d] Data from Ebert et al.[73] [e] Data from Ebert et al.[74] [f] Data from Ebert et al.[13] [g] Data from Ebert et al.,[75] [h] Antagonist K_i and pK_i values. [i] Data from Woodward et al.[15] using two-electrode voltage-clamp on Poly(A)$^+$ RNA from rat cortex expressed in *Xenopus* oocytes. [j] Data from Chebib et al.[76] using two-electrode voltage-clamp on human ρ_1 receptors expressed in *Xenopus* oocytes. [k] Data from Duke et al.[31] using two-electrode voltage-clamp on human ρ_1 receptors expressed in *Xenopus* oocytes. [l] Krehan et al.[28] [m] Data from Ragozzino et al.[17] using two-electrode voltage-clamp on Poly(A)$^+$ RNA from rat cortex expressed in *Xenopus* oocytes.

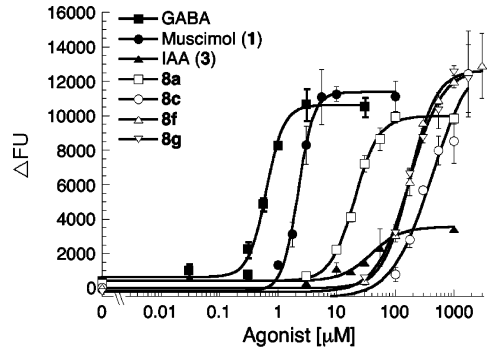

Figure 2. Concentration-response curves for GABA, muscimol (**1**), IAA (**3**), **8a**, **8c**, **8f**, and **8g** at a HEK293 cell line stably expressing the human ρ1 $GABA_C$ receptor in the FMP assay. The responses elicited by the compounds are given as ΔFU (fluorescent units), and data are the mean ± SD of duplicate determinations of single representative experiments.

3, illustrating our proposed binding modes for GABA and compound **8a** in the $GABA_A$ and $GABA_C$ receptors, respectively.

In our model of the orthosteric site of the $\alpha_1\beta_2\gamma_2$ $GABA_A$ receptor, the carboxylate group of GABA binds in a bidentate way to the α_1Arg66 residue.[39] This residue is conserved in all six $GABA_A$ α-subunits as well as in the ρ_1 $GABA_C$ subunit (Arg104). These arginines have in mutational studies been strongly implicated as binding partners to the carboxylate group of GABA in $GABA_A$[41,42] as well as in $GABA_C$ receptors.[23,43] The conformation of Arg66/Arg104 in the models (Figure 3) is in agreement with that required by our pharmacophore model for $GABA_A$ ligands.[39] The α_1Arg119 residue, which in our model is located close to α_1Arg66 have been mutated to lysine with a resulting significant increase in the EC_{50} for GABA.[44] The location of Arg119 and its conformational flexibility makes it possible for this residue to make additional stabilization of the binding of the anionic part of GABA (Figure 3a). Analogously, the corresponding residue in ρ_1Arg158 has been proposed to be involved in GABA binding on the basis of a mutagenesis study.[23]

In the proposed orientation in the $GABA_A$ receptor binding pocket, the ammonium group of GABA and the protonated imidazole ring of **8a** display cation−π interactions with the aromatic ring of β_2Tyr157 (Figure 3a). The distance between the ammonium nitrogen atom and the center of Tyr157 in Figure 3 is 5.1 Å, well within the limits for a cation−π interaction according to Gallavan et al.[45] A conservative mutation of this residue to phenylalanine significantly reduces the activity of GABA and muscimol consistent with an impairment of agonist binding, and mutation of the residue to a serine results in a 1000-fold reduced agonist activity.[46] In addition, the ammonium group of GABA and an imidazole N−H moiety in **8a** display a hydrogen bond (2.7 and 2.9 Å, respectively) to the backbone carbonyl group of β_2Tyr157. Thus, the cationic part of GABA is proposed to bind in a similar location and with similar interactions as the binding of the cationic parts of nicotinic agonists such as nicotine and epibatidine to the AChBP of *Lymnae stagnalis*[47] and *Aplysia californica*.[18] The cation−π interaction in the AChBP is provided by a tryptophan (Trp147) in a position equivalent to $GABA_A$ β_2Tyr157.

In the $GABA_C$ receptor, the residue Tyr198 is in a position equivalent to β_2Tyr157 in the $GABA_A$ receptor (Figure 3b). By use of unnatural amino acid mutagenesis with fluorinated phenylalanines, Tyr198 has unambiguously been shown to be involved in cation−π interactions, most likely to the ammonium group of GABA.[48] Recently, Pagdett et al., using the same mutagenesis method, surprisingly concluded that β_2Tyr97 (see Figure 3a) rather than β_2Tyr157 is the cation−π interaction partner to GABA in the $GABA_A$ binding pocket.[49] A cation−π interaction is unambiguously established for β_2Tyr97, but in our opinion it is not clear whether GABA is involved. As also noted by Padgett et al.,[49] this cation−π interaction may be due to interaction with some cationic moiety other than GABA. In our model, β_2Arg207 is in an ideal position for such an interaction and mutation of this residue to a cysteine has been

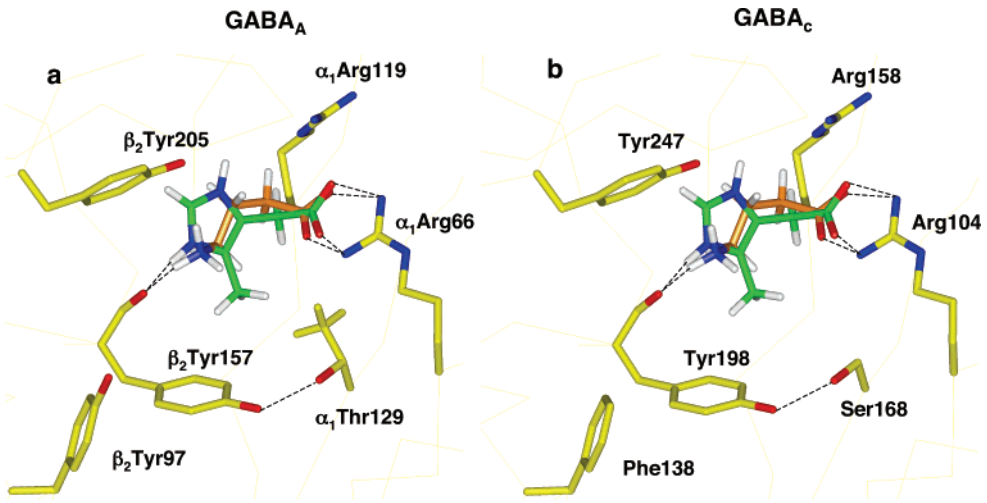

Figure 3. Ligand−receptor interaction models for the orthosteric sites of (a) $GABA_A$ receptor and (b) $GABA_C$ receptor. The ligands GABA and **8a** are shown using orange and green carbon atoms, respectively. Other atoms in the ligands are colored by atom type. Hydrogens other than those on the ligands are omitted for clarity. Proposed hydrogen bond interactions are shown as dashed lines.

shown to significantly reduce apparent GABA binding.[50] The corresponding amino acid residue in the ρ_1 $GABA_C$ receptor is also an arginine (Arg249). Unfortunately, Phe138 in ρ_1, which corresponds to β_2Tyr97 in $GABA_A$, has not been subjected to the same mutagenesis experiments with fluorinated aromatics as Tyr97. Such experiments may clarify if the orientations of GABA in the orthosteric sites of $GABA_A$ and $GABA_C$ receptors are different. The mutagenesis data for β_2Tyr157 are difficult to interpret in terms of possible cation−π interactions because of a surprisingly large increase in activity (467-fold) for the *p*-fluorophenylalanine mutant compared to the phenylalanine mutant.

According to our models (Figure 3), the main difference in the vicinity of the ligands in the orthosteric sites of the $\alpha_1\beta_2\gamma_2$ and ρ_1 receptors is the presence of a threonine residue (Thr129) in the α_1 subunit and a serine (Ser168) in the equivalent position in ρ_1. It has been shown in mutagenesis studies that α_1Thr129 lines the binding pocket of the $GABA_A$ receptor[42,51] and that the Ser168 residue plays an important role in the function of the $GABA_C$ receptor.[22,52] Mutational data indicate a hydrogen bond in the $GABA_A$ binding pocket between β_2Tyr157 and α_1-Thr129 with β_2Tyr157 as the hydrogen bond acceptor.[49] Harrison and Lummis have proposed a corresponding hydrogen bond between Ser168 and Tyr198 in the ρ_1 $GABA_C$ receptor.[43] These hydrogen bonds are shown in Figure 3. The hydrogen bond in the $GABA_A$ receptor (Figure 3a) positions the methyl group of the side chain of the α_1Thr129 residue such that it decreases the size of the binding pocket compared to the size of the binding pocket in the ρ_1 $GABA_C$ receptor (Figure 3b). In the model of the $\alpha_1\beta_2$ interface of the $GABA_A$ receptor, the 5-substituents in **8a**−**g** experience steric repulsions with this methyl group of α_1Thr129, as illustrated by the 5-methyl substituted IAA (**8a**) in Figure 3a. The distance between the interacting methyl groups in Figure 3a is 3.49 Å (carbon−carbon distance), and the distance between the closest hydrogen atoms is 1.79 Å. Energy calculations of the methyl−methyl interaction using the MM3 force field[53] and with the methyl groups in the relative positions as shown in Figure 3a indicate a repulsive interaction by 2.97 kcal/mol compared to two noninteracting methyl groups. This corresponds to a decrease in affinity by a factor of ~100, rationalizing the observed lower binding affinity displayed by **8a** compared to that of **4** at native $GABA_A$ receptors (Table 1) and the complete inactivity of the other 5-substituted IAA analogues (**8b**−**g**) at the receptors. It should be noted that the models in Figure 3 are homology models for which details such as the precise distances between groups and energy calculations should be viewed with due caution.

The smaller size of the side chain of the Ser186 residue in the ρ_1 receptor makes it possible for the orthosteric site in the $GABA_C$ receptor to accommodate substituents in the 5-position of IAA. In accordance with the virtually identical EC_{50} values exhibited by **4** and **8a** at the ρ_1 $GABA_C$ in the FMP assay, Ser168 provides sufficient space for the methyl group in **8a** (Table 1). In contrast, the larger iodine substituent in **8b** cannot be accommodated. Inspection of the interactions in the ρ_1 $GABA_C$ binding pocket for the phenyl group in **8c** and the para-substituted phenyl groups in **8f** and **8g** indicates that these substituents may also be fairly well accommodated with the phenyl group in an orthogonal conformation with respect to the imidazole ring (Figure 3b). In **8c**, the phenyl substituent must have an orthogonal orientation with respect to the imidazole ring. If the length of the phenyl group can be accommodated, the size of the phenyl group should be considered as the "thickness" of the phenyl substituent. Since the thickness of a phenyl ring is usually taken to be 3.4 Å, it is smaller than twice the van der Waals radius of an iodo substituent (4.0−4.7 Å). A similar strucuture−activity relationship has recently been observed by us for a chloro vs a phenyl substituent in a series of $GABA_A$ ligands.[54]

The 2-substituted compounds **8h**−**k** are all inactive at the $GABA_A$ receptor as well as at the $GABA_C$ receptor (Table 1). In our homology models, the 2-substituents of these compounds display strong steric repulsive interactions with β_2Tyr205 and ρ_1Tyr247 in the $GABA_A$ and $GABA_C$ receptor, respectively.

Thus, the models in Figure 3 are able to rationalize the observed pharmacological data in Table 1 and identify α_1Thr129 in $GABA_A$ and ρ_1Ser168 in $GABA_C$ as the major determinants for the selectivity displayed by the 5-substituted IAA analogues **8a**, **8c**, **8f**, and **8g** for $GABA_C$ over $GABA_A$.

Mutagenesis Study. To investigate whether the selectivity for $GABA_C$ over $GABA_A$ receptors displayed by the 5-substituted IAA analogues could be ascribed to a single amino acid residue; the Ser168 residue in the ρ_1 $GABA_C$ receptor and the corresponding Thr129 residue in the human α_1 $GABA_A$ receptor subunit, the ρ_1Ser168Thr and α_1Thr129Ser mutants were constructed.

The 5-substituted IAA analogues were characterized pharmacologically at tsA-201 cells transiently transfected with ρ_1-

Table 2. Functional Characteristics at WT or S168T ρ1 Receptors Transiently Expressed in tsA Cells in the FMP Assay[a]

	WT ρ_1		S168T ρ1	
	EC_{50} (μM)[b] [pEC_{50} ± SEM]	R_{max} ± SEM	EC_{50} (μM)[b] [pEC_{50} ± SEM]	R_{max} ± SEM
GABA	0.43 [6.4 ± 0.04]	100	22 [4.7 ± 0.03]	100
muscimol (**1**)	0.62 [6.2 ± 0.05]	104 ± 6	24 [4.6 ± 0.05]	96 ± 4
IAA (**4**)	5.5 [5.3 ± 0.03]	37 ± 4	~100[c]	~10[c]
8a	11 [5.0 ± 0.02]	106 ± 4	>1000	nd
8c	140 [3.8 ± 0.03]	131 ± 7	>3000	nd
8f	220 [3.7 ± 0.04]	127 ± 6	>3000	nd
8g	330 [3.5 ± 0.04]	94 ± 5	>3000	nd

[a] The R_{max} values are given as % of the maximal response of GABA at the respective receptors. The data are based on at least three individual experiments performed in duplicate. nd, not determinable. [b] EC_{50} values were calculated from pEC_{50} values found in brackets. [c] Because of the low efficacy of **4** at Ser168Thr ρ_1, the potency and maximal response of the compound are given as estimates.

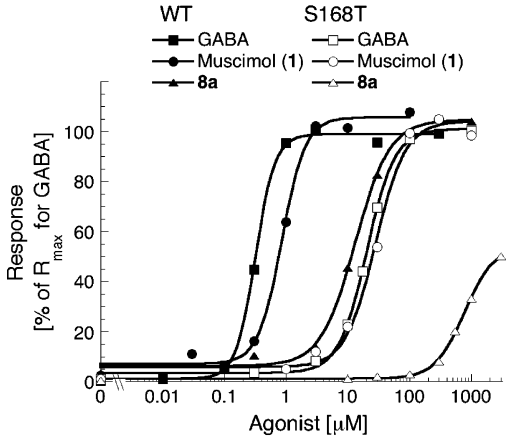

Figure 4. Concentration-response curves for GABA, muscimol (**1**), and **8a** at WT and Ser168T ρ1 receptors transiently expressed in tsA201 cells in the FMP assay. The responses elicited by the compounds are given as % of the R_{max} for GABA at the respective receptors. The data for the WT and the mutant ρ1 receptor are given as closed and open symbols, respectively. Data are given as the mean ± SD of duplicate determinations of single representative experiments.

WT or ρ_1Ser168Thr in the FMP assay. The functional properties of the analogues at the WT receptor transiently expressed in this cell line were in good agreement with those obtained at the stable ρ_1-HEK293 cell line (Table 2 and Figure 4). The substitution of Ser168 with Thr in the ρ_1 receptor resulted in dramatic reductions in the potencies for all the agonists tested (Figure 4). The potencies of standard GABA agonists GABA and **1** were reduced 40- to 50-fold at the mutant compared to the WT receptor, whereas **4**, **8a**, **8c**, **8f**, and **8g** displayed 20-, >100-, >20-, >10-, and >7-fold higher EC_{50} values, respectively, at the mutant compared to those obtained at the WT ρ_1 receptor. The functional properties of GABA, **4**, and **8a** were also characterized at the WT ρ_1 receptor transiently expressed in HEK293 cells using the patch-clamp technique (Table 3 and Figure 5). The ρ_1 receptor agonism displayed by compound **8a** in the FMP assay was verified at the human WT ρ_1 receptor in this conventional electrophysiological setup (Table 3). Compound **4** was found to be a low efficacious partial agonist at the receptor (R_{max} = 7.5%), and in concordance with the findings in the FMP assay compound **8a** (R_{max} = 66%) was found to be a more efficacious partial agonist than its parent compound (Table 3 and Figure 5).

To investigate whether the substitution of Thr129 in the α_1 subunit with a Ser residue could introduce a "ρ1-like" profile of the 5-substituted IAA analogue at the $\alpha_1\beta_2\gamma_{2S}$ $GABA_A$ receptor, the functional properties of GABA, **4**, and **8a** were also characterized at HEK293 cells transiently expressing WT $\alpha_1\beta_2\gamma_{2S}$ and mutant α_1(Thr129Ser)$\beta_2\gamma_{2S}$ receptors using the whole-cell patch-clamp technique. Introduction of the Thr129Ser mutation in the α_1 subunit of the rat $\alpha_1\beta_2\gamma_{2S}$ receptor resulted in significantly increased potencies for GABA and **4** compared to those at the WT $\alpha_1\beta_2\gamma_{2S}$ (Table 3 and Figure 5). In contrast, compound **8a** only elicited very small responses at the WT $\alpha_1\beta_2\gamma_{2S}$ and the α_1(Thr129Ser)$\beta_2\gamma_{2S}$ receptor at concentrations up to 1000 μM (Table 3 and Figure 5). The Hill coefficients for GABA at the WT $\alpha_1\beta_2\gamma_{2S}$, the α_1(Thr129Ser)$\beta_2\gamma_{2S}$ mutant, and the WT ρ_1 were 1.03, 1.03, and 2.1, respectively, reflecting the higher number of binding sites in the homomeric ρ_1 receptor than in the heteromeric $GABA_A$ receptor.

The deactivation kinetics observed for GABA were markedly slower at the WT ρ_1 receptor than at the WT $\alpha_1\beta_2\gamma_{2S}$ and α_1(Thr129Ser)$\beta_2\gamma_{2S}$ receptors. The slow deactivation of WT ρ_1 receptors has been attributed to a long lifetime of the open channel, which must close before GABA can dissociate.[55] It was therefore surprising that the deactivation of currents induced by compounds **8a** and **4** at the WT ρ_1 receptors was quite fast (completed within 10 s even at saturating concentrations) compared to that of GABA (completed within 1−2 min). The reasons for this interesting profile of the IAA analogues remain to be investigated.

Discussion

A high degree of amino acid sequence homology exists between the $GABA_A$ and $GABA_C$ receptor subunits, in particular when it comes to the orthosteric sites in the receptors because these sites have been under evolutionary pressure to remain able to bind GABA. As a consequence of this, ligands conventionally considered as prototypic $GABA_A$ receptor agonists, such as muscimol (**1**), isoguvacine (**2**), THIP (**3**), and IAA (**4**) all display activities at the $GABA_C$ receptors as well. The pharmacological profiles for these $GABA_A$ agonists span from being agonists, partial agonists, and antagonists at the $GABA_C$ receptors (Table 1).

In the present study compound **4**, a partial agonist at $GABA_A$ and $GABA_C$ receptors, has been used as a lead for studying its structure−activity relationships at the ionotropic GABA receptors. IAA (**4**) is a naturally occurring metabolite of histamine. The compound has various neurological effects believed to be mediated by the central $GABA_A$ receptors.[56] It penetrates the blood−brain barriers on systemic administration and is therefore advantageous from a bioavailability perspective compared to other known standard ligands for the ionotropic GABA receptors. In spite of this advantage in terms of drug delivery, **4** has attracted limited interest as a lead strucure and only very few studies on analogues of **4** as potential ligands for the ionotropic GABA receptors have been performed.[57,58]

In the present study, we have investigated the structure−activity relationships for 2- and 5-substituted IAA analogues at the $GABA_A$ and $GABA_C$ receptors. Introduction of even small substituents in the 2-position of **4** was found to have detrimental effects on the activities of **4** at both receptor classes, suggesting that there is little space in the orthosteric sites of both the $\alpha_1\beta_2\gamma_{2S}$ $GABA_A$ and the ρ_1 $GABA_C$ receptors around this position of the IAA molecule. The observed inactivity of the 2-substituted analogues is in accordance with the proposed position and orientation of the IAA molecule in the homology models of the orthosteric sites of the $\alpha_1\beta_2\gamma_{2S}$ $GABA_A$ and ρ_1 $GABA_C$ receptors (Figure 3).

In contrast to the lack of activity in the 2-substituted IAA analogues, several of the 5-substituted IAA analogues retained

Table 3. Functional Characteristics of $\alpha_1\beta_2\gamma_2$, α_1(Thr129Ser)$\beta_2\gamma_2$, and ρ1 Receptors Transiently Expressed in HEK-293 Cells Measured Using Whole-Cell Patch-Clamp[a]

	ρ_1			α_1T129S$\beta_2\gamma_2$			$\alpha_1\beta_2\gamma_2$		
	EC_{50} (μM)[b] (pEC_{50} ± SEM)	n_H ± SEM	R_{max} ± SEM	EC_{50} (μM)[b] (pEC_{50} ± SEM)	n_H ± SEM	R_{max} ± SEM	EC_{50} (μM)[b] (pEC_{50} ± SEM	n_H ± SEM	R_{max} ± SEM
GABA	6 (5.22 ± 0.03)	2.08 ± 0.23	100	12.8 (4.89 ± 0.04)	1.03 ± 0.07	100	43 (4.37 ± 0.06)	1.03 ± 0.012	100
IAA (**4**)	5.5 (5.26 ± 0.08)	0.92 ± 0.13	7.5 ± 2.4	20 (4.70 ± 0.03)	0.92 ± 0.05	39 ± 7	138 (3.86 ± 0.02)	1.17 ± 0.04	23 ± 4
8a	31 (4.50 ± 0.06)	1.06 ± 0.13	66 ± 9	>1000			>1000		

[a] R_{max} values are given in % of the maximal response of GABA. The data are based on at least five individual cells. [b] EC_{50} values were calculated from pEC_{50} values found in brackets.

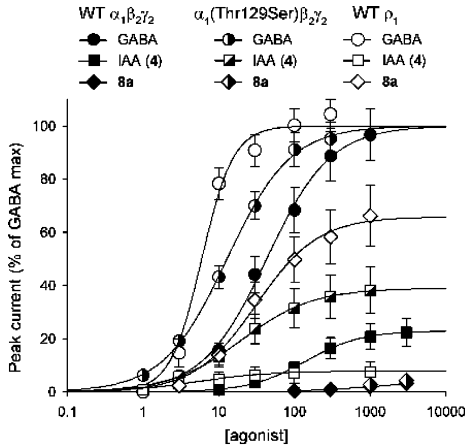

Figure 5. Concentration-response curves for GABA, IAA (**4**), and **8a** at $\alpha_1\beta_2\gamma_2$, α_1(Thr129Ser)$\beta_2\gamma_2$, and ρ_1 receptors transiently expressed in HEK-293 cells measured using whole-cell patch-clamp. The responses elicited by the compounds are given as % of the R_{max} for GABA at the respective receptors. The data for the $\alpha_1\beta_2\gamma_2$, α_1-(Thr129Ser)$\beta_2\gamma_2$. and ρ_1 receptors are given as closed, open/closed, and open symbols, respectively. Each point represents the mean ± SEM of five to seven different cells.

the agonist properties of **4** at ρ_1 $GABA_C$ receptor while exhibiting no measurable binding affinity to native $GABA_A$ receptors and no functional activities at the $\alpha_1\beta_2\gamma_{2S}$ $GABA_A$ receptor subtype (Table 1). The 5-substituted IAA analogues **8a**,**c**,**f**,**g** exhibited agonist potencies on the ρ_1 receptor similar to or up to 30-fold lower than that of **4**. Thus, there appears to be ample space in the orthosteric site of the ρ_1 receptor to accommodate the binding of 5-substituted IAA analogues. In fact, the cavity or gap surrounding the 5-position of IAA is clearly large enough to encompass a phenyl ring with a para substituent but not phenyl rings with ortho or meta substituents. This can be rationalized by the presence of repulsive steric interactions between the 5-substituent and the methyl group of the side chain of the α_1Thr129 residue in the $GABA_A$ receptor, whereas the smaller side chain of the Ser168 residue in the corresponding position in the ρ_1 $GABA_C$ receptor allows binding of the 5-substituents in **8a**, **8c**, **8f**, and **8g** (Figure 3).

The functional characterization of the IAA analogues at the ρ_1 $GABA_C$ receptor was performed using the fluorescence-based FMP assay. This assay has previously been applied in studies of other ligand-gated ion channels, where the functional properties determined for the receptors have been in good agreement with those obtained in conventional electrophysiological setups.[59−61] The functional characteristics displayed by the ρ_1-HEK293 cell line in the FMP assay were found to be in reasonable agreement with the findings of previous electrophysiology studies. In the FMP assay GABA displayed an EC_{50} value around 1 μM at ρ_1, which is similar to the potencies observed for the endogenous agonist in electrophysiological studies of the receptor expressed in *Xenopus* oocytes.[62−64] Furthermore, the standard agonists **1**, **2**, and **4** displayed agonist potencies 4-fold lower, 120-fold lower, and 24-fold lower potencies, respectively, than GABA at the receptor, and this rank order is also in concordance with the literature.[62−64] Finally, the high and low micromolar EC_{50} values exhibited by the competitive $GABA_C$ antagonists THIP (**3**) and TPMPA (**7**), respectively, are also similar to previous reported values.[63] While the agonist and antagonist potencies obtained in the FMP assay thus correlated well with the literature, the maximal responses displayed by standard agonists **1**, **2**, and **4** compared to GABA were somewhat higher than those reported previously for the agonists. For example, in contrast to the full agonism displayed by both **1** and **2** and the efficacy of 32% displayed by **4** in the FMP assay, **1**, **2**, and **4** have in previous studies of the ρ_1 receptor expressed in *Xenopus* oocytes displayed efficacies of 76−88%, 45−47%, and 3−9%, respectively.[62−64] Furthermore, in patch-clamp recordings at ρ_1 expressing HEK293 cells, we determined the maximal response of **4** to be 7.5% of that of GABA (Table 3 and Figure 5). We have observed a similar apparent overestimation of the maximal response of the partial agonist taurine at an α_1 glycine receptor cell line in the FMP assay.[61] Although the efficacies determined for the 5-substituted IAA analogues in the FMP assay thus might be higher than if the analogues had been characterized in a conventional electrophysiology setup, the rank order of efficacies displayed by GABA, **4**, and **8a** (GABA ≥ **8a** > **4**) was the same in the FMP assay and in the patch clamp recordings (Figures 2 and 5). Thus, it is clear that introduction of substituents in the 5-position of **4** results in significant increases in the efficacy of the agonist. We have not characterized the functional properties of the 5-Ph, 5-*p*-Me-Ph, or 5-*p*-F-Ph analogues, **8c**,**f**,**g**, at ρ_1 in the patch-clamp setup, but on the basis of the FMP data, it appears (Tables 1 and 2) that the efficacies of these analogues may be even further increased compared to **4** than the 5-Me-IAA analogue **8a**.

The Ser168Thr mutation in the ρ_1 subunit of the $GABA_C$ receptor gives rise to an almost " $GABA_A$-like" profile for the 5-substituted IAA analogues **8a**,**c**,**f**,**g** as well as for standard agonists GABA, **1**, and **4** (Tables 1 and 2). Although the potencies of all three agonists were significantly decreased at the Ser168Thr mutant, the fact that the mutation has a significantly larger impact on the potency of **8a** than on that of **4** seems to suggest that the Ser168 residue is a major determinant for the selectivity of **8a** for the $GABA_C$ receptor over the $GABA_A$ receptor.

On the basis of the functional agonist characteristics of the WT and Ser168Thr ρ_1 receptors and the homology models of the orthosteric site of the $\alpha_1\beta_2\gamma_{2S}$ $GABA_A$ receptor, we expected that introduction of a Thr129Ser mutation in α_1GABA_A would increase the agonist potencies of the 5-substituted IAA analogues at the $\alpha_1\beta_2\gamma_{2S}$ receptor. However, whereas GABA and **4**

displayed increased potencies at the α_1(Thr129Ser)$\beta_2\gamma_{2S}$ mutant compared to the WT receptor, compound **8a** was unable to elicit responses through neither of the receptors at concentrations up to 1 mM (Figure 5). This observation does not exclude the possibility that the agonist potency of **8a** could in fact be increased at the α_1(Thr129Ser)$\beta_2\gamma_{2S}$ mutant compared to the WT receptor. However, since we are not able to test the compound at concentrations higher than 1 mM, the results on **8a** at the WT and mutant $\alpha_1\beta_2\gamma_{2S}$ must be said to be nonconclusive. Nevertheless, the ρ_1Ser168/α_1Thr129 residues appear to be a general determinant of the observed differences in agonist potencies at the $GABA_A$ and $GABA_C$ receptors.

Conclusion

In summary, a series of ring-substituted IAA analogues have been synthesized and characterized pharmacologically at $GABA_A$ and $GABA_C$ receptors using a fluorescence-based assay and electrophysiological techniques. All of the synthesized compounds **8a**−**l** were inactive at native $GABA_A$ receptors and at recombinant $\alpha_1\beta_2\gamma_{2S}$ $GABA_A$ receptors. Whereas the 2-substituted IAA analogues **8h**−**l** were inactive at the ρ_1 $GABA_C$ receptors, the 5-Me, 5-Ph, 5-*p*-Me-Ph, and 5-*p*-F-Ph-IAA analogues, **8a**,**c**,**f**,**g**, displayed agonist potencies at the receptor similar to or 30-fold lower than that of the parent compound **4**. Furthermore, the IAA analogues were high efficacious partial agonists or full agonists at the $GABA_C$ receptor, contrasting with the low efficacy of **4**. Most notably, the present work has led to the selective efficacious $GABA_C$ receptor agonist, compound **8a**, which could become an important tool for further pharmacological investigations of the $GABA_C$ receptors. Similar to the standard $GABA_C$ agonist (+)-CAMP (**6**), **8a** displays mid-micromolar EC_{50} values at the ρ_1 receptor. However, in contrast to (+)-CAMP, **8a** does not display measurable activity at the $\alpha_1\beta_2\gamma_{2S}$ $GABA_A$ receptor at concentrations up to 1 mM.

The molecular basis for the observed $GABA_A$/$GABA_C$ selectivity of **8a** has been addressed in a mutagenesis study based on ligand−receptor docking experiments using a homology model for the $GABA_A$ receptor. In this study the Thr129 residue in the α_1 subunit of the $\alpha_1\beta_2\gamma_{2S}$ $GABA_A$ receptor and the corresponding Ser168 residue in the ρ_1 receptor have been identified as major molecular determinants for the observed differences in agonist potencies between the two receptors.

Experimental Section

Chemistry. General Procedures. Chloromethyl benzyl ether[65] (*caution: toxic and carcinogenic*) and 4,5-diiodoimidazole[33] were prepared according to literature procedures. All other chemicals were >95% pure from commercial suppliers and used as received unless otherwise stated. All reactions using moisture- and/or air-sensitive reagent(s) were carried out in flame- or oven-dried glassware under a nitrogen or argon atmosphere. Unless otherwise stated, dry THF, Et_3N, and DMF were obtained by storage over activated sieves (4 Å) to a water content below 20 ppm, measured on a Metrohm 737 KF coulometer. TLC was run on Merck silica gel 60 F_{254} plates, and compounds were visualized using $KMnO_4$ spraying reagent and UV light. Dry column vacuum chromatography[66] (DCVC) was performed using Merck 15111 silica gel 60 (0.015−0.040 mm) using 0−100% EtOAc in petroleum spirit 80−100 (v/v), with increments of 5%. If necessary, this was followed by 1−20% CH_3OH in EtOAc (v/v), with increments of 1%. Reverse-phase chromatography (RPC) was performed using Merck LiChroprep RP-18 (40−63 μM). ^{1}H NMR spectra were recorded on a Varian Gemini 2000 (300 MHz), Varian Mercury Plus (300 MHz), or Bruker Avance (500 MHz) instrument, and the data are tabulated in the following order: chemical shift (δ) [multiplicity (br, broad; s, singlet; d, doublet; t, triplet; q, quartet; dd, doublet of doublets; m, multiplet), coupling constant(s) J (Hz), number of protons]. Tetramethylsilane was used as internal reference in $CDCl_3$ ($\delta_H = 0$). In DMSO-d_6 and CD_3OD the solvent residual peak (δ_H = 2.50 and 3.31, respectively) was used as internal reference.[67] ^{13}C NMR spectra were recorded on the same instruments using the central signals of $CDCl_3$ ($\delta_C = 77.16$), DMSO-d_6 ($\delta_C = 39.52$), and CD_3OD ($\delta_C = 49.00$) as reference signals.[67] ^{19}F NMR spectra were recorded on a Bruker Avance (500 MHz) instrument with $CFCl_3$ as external reference. Low-resolution MS (EI) data were obtained on a Shimadzu GCMS-QP5050A. Low-resolution MS (APPI) data were obtained on a Sciex API150ex analytical LC/MS. High-resolution MS data were obtained on a JEOL HX 110/110 mass spectrometer at Mass Spectrometry Research Unit, Department of Chemistry, University of Copenhagen, Denmark. The expected isotope patterns were always observed in the mass spectra. Elemental analyses were performed at Analytical Research Department, H. Lundbeck A/S, Denmark, or by J. Theiner, Department of Physical Chemistry, University of Vienna, Austria. Melting points were determined in capillary tubes and are uncorrected. *E*/*Z* ratios were determined by ^{1}H NMR. The analytical data obtained for compounds previously published are in agreement with the data reported.

1-(Benzyloxy)methyl-5-formyl-4-iodoimidazole (9). 9 was prepared from 1-(benzyloxy)methyl-4,5-diiodoimidazole as described by Carver et al.[33] with the following modifications: The concentration of the starting material in dry THF was 0.075 mmol/mL, ^{i}PrMgCl (2M in THF) was used as base, and DMF was used as electrophile. This resulted in **9** being isolated in 75% yield as pale-yellow crystals: mp 43−45 °C.

***E*/*Z*-1-(Benzyloxy)methyl-4-iodo-5-(2-methoxyethenyl)imidazole (10).** (Methoxymethyl)triphenylphosphonium chloride (1.7 g, 4.9 mmol, dried azeotropically with toluene) was suspended in dry THF (50 mL) and cooled to 0 °C. NaHMDS (2 M in THF, 2.5 mL, 4.9 mmol) was added dropwise, and the resulting red suspension was stirred for 2 h at room temperature. **9** (1.3 g, 3.8 mmol, dried azeotropically with toluene) was dissolved in dry THF (6 mL), and this solution was added dropwise at 0 °C. The reaction mixture was slowly heated to room temperature, stirred for 20 h, and cooled to 0 °C followed by addition of saturated aqueous NH_4Cl and H_2O (1:1, 50 mL). The resulting mixture was stirred vigorously and then extracted three times with EtOAc. The combined organic phases were washed with brine, dried ($MgSO_4$), and evaporated in vacuo. DCVC afforded **10** (1.2 g, 87%) as a pale-yellow oil. The formed *E* and *Z* isomers were not separated but isolated in a 10:7 ratio (*E*:*Z*), R_f = 0.71, 0.64/EtOAc. *E*-isomer, NMR ($CDCl_3$): δ_H 7.46 (s, 1H), 7.38−7.23 (m, 5H), 7.18 (d, J = 13.2, 1H), 5.51 (d, J = 13.2, 1H), 5.23 (s, 2H), 4.45 (s, 2H), 3.67 (s, 3H) ppm. *Z*-isomer, NMR ($CDCl_3$): δ_H 7.51 (s, 1H), 7.38−7.23 (m, 5H), 6.18 (d, J = 6.8, 1H), 5.10 (d, J = 6.8, 1H), 5.30 (s, 2H), 4.38 (s, 2H), 3.68 (s, 3H) ppm. Both isomers, NMR ($CDCl_3$): δ_C 152.8, 149.4, 138.7, 136.0, 135.6, 130.2, 129.6, 128.3, 128.24, 128.19, 127.9, 127.8, 127.54, 127.46, 91.8, 90.8, 85.8, 83.0, 74.5, 73.4, 69.8, 69.6, 60.1, 56.5 ppm. MS (EI): m/z 370 $[M]^{+\bullet}$. Anal. ($C_{14}H_{15}N_2O_2I$) C, H, N.

General Procedure for Suzuki Cross-Coupling of 10 into 11c−**i.** A solution of **10** (1 equiv), the appropriate boronic acid (2 equiv), and K_3PO_4 (3 equiv) in H_2O (8 mL/g **10**) and 1,4-dioxane (42 mL/g **10**) was degassed with argon for 2 h. $Pd(PPh_3)_2Cl_2$ (0.1 equiv) was added. The reaction mixture was heated to 110 °C for 17 h and then cooled to room temperature. EtO_2 was added, and the resulting solution was washed with H_2O, twice with 2 M NaOH (aq) and then with H_2O again. The organic phase was dried ($MgSO_4$) and evaporated in vacuo. DCVC of the residue afforded the desired product (**11**) as a mixture of the *E*- and *Z*-isomers, which were not separated.

***E*/*Z*-1-(Benzyloxy)methyl-5-(2-methoxyethenyl)-4-phenylimidazole (11c).** Preparation was done according to the general procedure using **10** (0.90 g, 2.4 mmol) and benzeneboronic acid to afford **11c** (0.57 g, 73%) as a brown oil. The two isomers were isolated in a 11:7 ratio (*E*:*Z*), R_f = 0.61, 0.42/EtOAc. *E*-isomer, NMR ($CDCl_3$): δ_H 7.83−7.76 (m, 2H), 7.54 (s, 1H), 7.38−7.18

(m, 8H), 6.92 (d, J = 13.2, 1H), 5.70 (d, J = 12.9, 1H), 5.23 (s, 2H), 4.51 (s, 2H), 3.65 (s, 3H) ppm. *Z*-isomer, NMR ($CDCl_3$): δ_H 7.83−7.76 (m, 2H), 7.61 (s, 1H), 7.38−7.18 (m, 8H), 6.18 (d, J = 6.6, 1H), 5.36 (d, J = 6.6, 1H), 5.30 (s, 2H), 4.41 (s, 2H), 3.54 (s, 3H) ppm. Both isomers, NMR ($CDCl_3$): δ_C 152.7, 149.6, 138.4, 137.2, 137.2, 136.4, 136.1, 135.0, 134.8, 131.8, 128.4, 128.3, 128.1, 128.0, 127.9, 127.8, 127.7, 127.7, 126.9, 126.4, 126.3, 126.1, 123.6, 121.8, 93.4, 91.9, 74.1, 73.0, 69.8, 69.6, 60.1, 56.6 ppm. MS (EI): m/z 320 $[M]^{+\bullet}$.

***E*/*Z*-1-(Benzyloxy)methyl-5-(2-methoxyethenyl)-4-(2-methylphenyl)imidazole (11d).** Preparation was done according to the general procedure using **10** (3.3 g, 8.8 mmol) and 2-methylbenzeneboronic acid to afford **11d** (2.3 g, 77%) as an orange oil. The two isomers were isolated in a 10:7 ratio (*E*:*Z*), R_f = 0.48, 0.40/EtOAc. *E*-isomer, NMR ($CDCl_3$): δ_H 7.55 (s, 1H), 7.38−7.28 (m, 6H), 7.24−7.13 (m, 3H), 6.62 (d, J = 13.0, 1H), 5.58 (d, J = 13.0, 1H), 5.29 (s, 2H), 4.53 (s, 2H), 3.51 (s, 3H), 2.28 (s, 3H) ppm. *Z*-isomer, NMR ($CDCl_3$): δ_H 7.62 (s, 1H), 7.38−7.28 (m, 6H), 7.24−7.13 (m, 3H), 5.98 (d, J = 6.8, 1H), 5.35 (s, 2H), 5.18 (d, J = 6.8, 1H), 4.46 (s, 2H), 3.31 (s, 3H), 2.32 (s, 3H) ppm. Both isomers, NMR ($CDCl_3$): δ_C 151.2, 148.4, 140.3, 138.3, 137.0, 136.9, 136.7, 136.6, 136.3, 135.2, 134.6, 130.5, 130.2, 130.0, 129.7, 128.5, 128.4, 128.1, 128.0, 127.8, 127.4, 127.0, 126.9, 125.8, 125.4, 124.8, 124.6, 123.3, 93.0, 91.8, 74.2, 73.4, 69.8, 69.7, 59.6, 56.3, 20.1, 20.0 ppm. MS (APPI): m/z 335 $[M + H]^+$.

***E*/*Z*-1-(Benzyloxy)methyl-5-(2-methoxyethenyl)-4-(3-methylphenyl)imidazole (11e).** Preparation was done according to the general procedure using **10** (3.6 g, 9.6 mmol) and 3-methylbenzeneboronic acid to afford **11e** (2.2 g, 70%) as an orange oil. The two isomers were isolated in a 21:19 ratio (*E*:*Z*), R_f = 0.53, 0.44/EtOAc. *E*-isomer, NMR ($CDCl_3$): δ_H 7.66 (br s, 1H), 7.58 (br d, J = 7.3, 1H), 7.55 (s, 1H), 7.36−7.22 (m, 6H), 7.04 (br d, J = 7.7, 1H), 6.94 (d, J = 13.0, 1H), 5.72 (d, J = 13.2, 1H), 5.24 (s, 2H), 4.51 (s, 2H), 3.65 (s, 3H), 2.37 (s, 3H) ppm. *Z*-isomer, NMR ($CDCl_3$): δ_H 7.71 (br s, 1H), 7.62 (s, 1H), 7.61 (br d, J = 8.4, 1H), 7.36−7.22 (m, 6H), 7.06 (br d, J = 8.2, 1H), 6.19 (d, J = 6.8, 1H), 5.37 (d, J = 6.8, 1H), 5.31 (s, 2H), 4.41 (s, 2H), 3.55 (s, 3H), 2.37 (s, 3H) ppm. Both isomers, NMR ($CDCl_3$): δ_C 152.7, 149.6, 138.7, 138.6, 137.8, 137.4, 137.3, 137.2, 136.6, 136.3, 135.0, 134.8, 128.5, 128.5, 128.4, 128.0, 128.0, 127.9, 127.8, 127.7, 127.7, 127.2, 127.0, 125.5, 124.0, 123.6, 123.6, 121.8, 93.6, 92.1, 74.1, 73.1, 69.8, 69.6, 60.0, 56.5, 21.3 ppm. MS (APPI): m/z 335 $[M + H]^+$.

***E*/*Z*-1-(Benzyloxy)methyl-5-(2-methoxyethenyl)-4-(4-methylphenyl)imidazole (11f).** Preparation was done according to the general procedure using **10** (2.5 g, 6.6 mmol) and 4-methylbenzeneboronic acid to give **11f** (1.7 g, 74%) as an orange oil. The two isomers were isolated in a 14:11 ratio (*E*:*Z*), R_f = 0.50, 0.42/EtOAc. *E*-isomer, NMR ($CDCl_3$): δ_H 7.68 (d, J = 8.0, 2H), 7.57 (s, 1H), 7.37−7.27 (m, 5H), 7.19 (d, J = 8.5, 2H), 6.93 (d, J = 13.0, 1H), 5.71 (d, J = 13.0, 1H), 5.26 (s, 2H), 4.53 (s, 2H), 3.66 (s, 3H), 2.36 (s, 3H) ppm. *Z*-isomer, NMR ($CDCl_3$): δ_H 7.72 (d, J = 8.0, 2H), 7.64 (s, 1H), 7.37−7.27 (m, 5H), 7.17 (d, J = 8.5, 2H), 6.20 (d, J = 6.6, 1H), 5.37 (d, J = 6.6, 1H), 5.32 (s, 2H), 4.43 (s, 2H), 3.57 (s, 3H), 2.36 (s, 3H) ppm. Both isomers, NMR ($CDCl_3$): δ_C 152.8, 149.6, 138.8, 138.7, 137.3, 137.3, 136.6, 136.3, 136.2, 135.9, 132.3, 132.1, 129.0, 128.7, 128.6, 128.5, 128.2, 128.0, 127.9, 127.9, 127.0, 126.5, 124.8, 123.4, 121.5, 93.8, 92.2, 74.2, 73.2, 69.9, 69.7, 60.1, 56.6, 21.1 ppm. HRMS (EI): m/z 334.1670 (calcd $C_{21}H_{22}N_2O_3$, 334.1681).

***E*/*Z*-1-(Benzyloxy)methyl-4-(4-fluorophenyl)-5-(2-methoxyethenyl)imidazole (11g).** Preparation was done according to the general procedure using **10** (2.6 g, 6.9 mmol) and 4-fluorobenzeneboronic acid to give **11g** (1.7 g, 71%) as an orange oil. The two isomers were isolated in a 10:8 ratio (*E*:*Z*), R_f = 0.48, 0.40/EtOAc. *E*-isomer, NMR ($CDCl_3$): δ_H 7.77 (dd, J = 12.9, J = 8.9, 2H), 7.57 (s, 1H), 7.39−7.28 (m, 5H), 7.07 (dd, J = 8.9, J = 2.0, 2H), 6.90 (d, J = 12.9, 1H), 5.67 (d, J = 12.9, 1H), 5.27 (s, 2H), 4.54 (s, 2H), 3.67 (s, 3H) ppm. *Z*-isomer, NMR ($CDCl_3$): δ_H 7.76 (dd, J = 12.7, J = 8.9, 2H), 7.63 (s, 1H), 7.39−7.28 (m, 5H), 7.03 (dd, J = 8.9, J = 2.1, 2H), 6.21 (d, J = 6.6, 1H), 5.34 (d, J = 6.6, 1H), 5.32 (s, 2H), 4.45 (s, 2H), 3.56 (s, 3H) ppm. Both isomers, NMR ($CDCl_3$): δ_C 162.7, 162.6, 160.6, 153.2, 150.0, 138.0, 137.8, 137.4, 137.3, 136.5, 136.3, 131.5, 131.4, 131.1, 131.1, 128.7, 128.7, 128.6, 128.5, 128.2, 128.2, 128.1, 127.9, 127.9, 123.6, 121.7, 115.2, 115.1, 114.8, 114.6, 93.2, 91.8, 74.1, 73.2, 69.9, 69.8, 60.1, 56.7 ppm. δ_F 61.1, 60.7 ppm. HRMS (EI): m/z 338.1432 (calcd $C_{20}H_{19}N_2O_2F$, 338.1431).

***E*/*Z*-1-(Benzyloxy)methyl-2-chloro-5-(2-methoxyethenyl)-4-phenylimidazole (14h).** A solution of **11c** (1.7 g, 5.2 mmol, dried azeotropically with toluene) in dry THF (75 mL) was cooled to −78 °C followed by dropwise addition of *n*-BuLi (1.6 M in hexane, 5.46 mmol). After the mixture was stirred at −78 °C for 15 min, a solution of C_2Cl_6 (1.7 g, 7.3 mmol) in dry THF (3 mL) was added dropwise. The mixture was allowed to reach room temperature and stirred for further 5 h. Saturated aqueous NH_4Cl and H_2O (1:1, 200 mL) were added, and the resulting mixture was extracted three times with EtOAc. The combined organic phases were washed with brine, dried ($MgSO_4$), and evaporated. DCVC of the residue afforded **14h** (1.7 g, 91%) as a yellow oil. The product was isolated as a mixture of the *E*- and *Z*-isomers in a 13:9 ratio (*E*:*Z*), R_f = 0.38, 0.32/(1:2 EtOAc/*n*-heptane), which were not separated. *E*-isomer, NMR ($CDCl_3$): δ_H 7.79−7.75 (m, 2H), 7.38−7.22 (m, 8H), 6.91 (d, J = 13.2, 1H), 5.65 (d, J = 13.0, 1H), 5.34 (s, 2H), 4.63 (s, 2H), 3.67 (s, 3H) ppm. *Z*-isomer, NMR ($CDCl_3$): δ_H 7.79−7.75 (m, 2H), 7.38−7.22 (m, 8H), 6.23 (d, J = 6.6, 1H), 5.37 (s, 2H), 5.36 (d, J = 6.3, 1H), 4.51 (s, 2H), 3.56 (s, 3H) ppm. Both isomers, NMR ($CDCl_3$): δ_C 153.9, 150.6, 137.6, 137.2, 136.8, 136.6, 134.3, 134.0, 132.5, 132.1, 128.5, 128.4, 128.3, 128.1, 129.0, 128.0, 127.7, 127.7, 127.1, 126.9, 126.7, 126.6, 125.7, 123.7, 93.3, 91.8, 73.3, 72.8, 70.5, 70.4, 60.2, 56.7 ppm. MS (APPI): m/z 355 $[M + H]^+$. Anal. ($C_{20}H_{19}N_2O_2Cl$) C, H, N.

***E*/*Z*-1-(Benzyloxy)methyl-5-(2-methoxyethenyl)-2-methyl-4-phenylimidazole (14i).** A solution of **11c** (2.0 g, 6.1 mmol, dried azeotropically with toluene) in dry THF (75 mL) was cooled to −78 °C followed by dropwise addition of *n*-BuLi (1.6 M in hexane, 6.4 mmol). After the mixture was stirred at −78 °C for 15 min, CH_3I (1.2 g, 8.5 mmol) was added dropwise. The mixture was allowed to reach room temperature and stirred for further 18 h. Saturated aqueous NH_4Cl and H_2O (1:1, 200 mL) were added, and the resulting mixture was extracted three times with EtOAc. The combined organic phases were washed with brine, dried ($MgSO_4$), and evaporated in vacuo. DCVC of the residue afforded **14i** (1.6 g, 80%) as an orange oil. The product was isolated as a mixture of the *E*- and *Z*-isomers in a 6:5 ratio (*E*:*Z*), R_f = 0.55, 0.47/EtOAc, which were not separated. *E*-isomer, NMR ($CDCl_3$): δ_H 7.81−7.77 (m, 2H), 7.38−7.18 (m, 8H), 6.75 (d, J = 13.0, 1H), 5.61 (d, J = 13.2, 1H), 5.22 (s, 2H), 4.54 (s, 2H), 3.63 (s, 3H), 2.46 (s, 3H) ppm. *Z*-isomer, NMR ($CDCl_3$): δ_H 7.81−7.77 (m, 2H), 7.38−7.18 (m, 8H), 6.17 (d, J = 6.6, 1H), 5.34 (d, J = 6.8, 1H), 5.29 (s, 2H), 4.42 (s, 2H), 3.55 (s, 3H), 2.49 (s, 3H) ppm. Both isomers, NMR ($CDCl_3$): δ_C 153.1, 149.6, 145.6, 145.1, 137.0, 136.7, 136.3, 135.3, 135.1, 128.6, 128.5, 128.4, 128.2, 128.1, 127.9, 127.9, 127.7, 127.6, 127.1, 126.6, 126.2, 126.1, 124.7, 123.5, 122.0, 94.3, 92.3, 72.9, 72.1, 69.8, 60.1, 56.6, 13.6, 13.5 ppm. HRMS (EI): m/z 334.1669 (calcd $C_{21}H_{22}N_2O_2$, 334.1681).

General Procedure for Hydrolysis of the Enol Ethers 10, 11c−i, and 14h,i. The enol ether was dissolved in 1,4-dioxane, and 6 M HCl (aq) (50 equiv) was added. The reaction mixture was heated to 70 °C for 20 min, cooled to room temperature, and poured into saturated aqueous $NaHCO_3$ (pH 8) followed by three extractions with EtOAc. The combined organic phases were washed with brine, dried ($MgSO_4$), and evaporated in vacuo. DCVC furnished the aldehyde.

1-(Benzyloxy)methyl-5-(formylmethyl)-4-iodoimidazole (12b). Preparation was done according to the general procedure from **10** (1.0 g, 2.8 mmol) to give **12b** (0.79 g, 78%) as colorless crystals: mp 105−107 °C, R_f = 0.58/EtOAc. NMR ($CDCl_3$): δ_H 9.62 (s, 1H), 7.53 (s, 1H), 7.41−7.33 (m, 3H), 7.27−7.24 (m, 2H), 5.24 (s, 2H), 4.40 (s, 2H), 3.81 (s, 2H) ppm. δ_C 195.8, 139.7, 135.3, 128.6, 128.4, 127.9, 126.1, 88.2, 74.1, 70.0, 39.8 ppm. MS (APPI): m/z 357 $[M + H]^+$. Anal. ($C_{13}H_{13}N_2O_2I$) C, H, N.

1-(Benzyloxy)methyl-5-(formylmethyl)-4-phenylimidazole (12c). Preparation was done according to the general procedure from **11c** (1.5 g, 4.7 mmol) to give **12c** (1.1 g, 79%) as a yellow oil. R_f = 0.35/EtOAc. NMR ($CDCl_3$): δ_H 9.68 (t, J = 1.4, 1H), 7.60 (s, 1H), 7.51−7.47 (m, 2H), 7.39−7.23 (m, 8H), 5.24 (s, 2H), 4.42 (s, 2H), 3.91 (d, J = 1.4, 2H) ppm. δ_C 197.0, 142.0, 138.0, 135.5, 133.3, 131.8, 128.6, 128.5, 128.3, 128.0, 127.4, 118.7, 74.0, 69.9, 39.0 ppm. MS (EI): m/z 306 $[M]^{+\bullet}$.

1-(Benzyloxy)methyl-5-(formylmethyl)-4-(2-methylphenyl)-imidazole (12d). Preparation was done according to the general procedure from **11d** (2.1 g, 6.2 mmol) to give **12d** (1.5 g, 76%) as a yellow syrup, R_f = 0.33/EtOAc. NMR ($CDCl_3$): δ_H 9.59 (t, J = 1.4, 1H), 7.62 (s, 1H), 7.39−7.23 (m, 7H), 7.20−7.15 (m, 2H), 5.28 (s, 2H), 4.47 (s, 2H), 3.72 (d, J = 1.4, 2H), 2.29 (s, 3H) ppm. δ_C 197.3, 142.9, 137.8, 137.6, 135.9, 133.1, 130.4, 130.2, 128.7, 128.3, 128.0, 125.5, 119.5, 74.1, 69.9, 38.7, 20.1 ppm. MS (APPI): m/z 321 $[M + H]^+$. Anal. ($C_{20}H_{20}N_2O_2$) C, H, N.

1-(Benzyloxy)methyl-5-(formylmethyl)-4-(3-methylphenyl)-imidazole (12e). Preparation was done according to the general procedure from **11e** (1.6 g, 4.7 mmol) to give **12e** (1.1 g, 75%) as an orange syrup, R_f = 0.34/EtOAc. NMR ($CDCl_3$): δ_H 9.72 (s, 1H), 7.59 (s, 1H), 7.43 (s, 1H), 7.38−7.26 (m, 7H), 7.13 (d, J = 6.4, 1H), 5.27 (s, 2H), 4.45 (s, 2H), 3.95 (s, 2H), 2.39 (s, 3H) ppm. δ_C 197.4, 142.5, 138.3, 137.9, 135.8, 133.8, 128.7, 128.4, 128.4, 128.1, 128.1, 128.1, 124.2, 118.5, 73.8, 69.8, 39.1, 21.4 ppm. MS (APPI): m/z 321 $[M + H]^+$. Anal. ($C_{20}H_{20}N_2O_2$) C, H, N.

1-(Benzyloxy)methyl-5-(formylmethyl)-4-(4-methylphenyl)-imidazole (12f). Preparation was done according to the general procedure from **11f** (1.5 g, 4.5 mmol) to give **12f** (1.1 g, 75%) as an orange syrup, R_f = 0.34/EtOAc. NMR ($CDCl_3$): δ_H 9.68 (s, 1H), 7.56 (s, 1H), 7.44 (d, J = 8.0, 2H), 7.36−7.29 (m, 3H), 7.26−7.24 (m, 2H), 7.20 (d, J = 8.0, 2H), 5.23 (s, 2H), 4.41 (s, 2H), 3.91 (s, 2H), 2.35 (s, 3H) ppm. δ_C 197.3, 142.2, 137.7, 136.9, 135.8, 131.0, 129.2, 128.5, 128.2, 127.9, 127.0, 118.1, 73.7, 69.7, 38.9, 21.0 ppm. MS (APPI): m/z 321 $[M + H]^+$.

1-(Benzyloxy)methyl-4-(4-fluorophenyl)-5-(formylmethyl)imidazole (12g). Preparation was done according to the general procedure from **11g** (1.6 g, 4.6 mmol) to give **12g** (1.2 g, 77%) as a yellow syrup, R_f = 0.33/EtOAc. NMR ($CDCl_3$): δ_H 9.69 (s, 1H), 7.57 (s, 1H), 7.51 (dd, J = 8.5, J = 5.4, 2H), 7.37−7.30 (m, 3H), 7.27−7.25 (m, 2H), 7.07 (dd, J = 8.9, J = 8.5, 2H), 5.25 (s, 2H), 4.43 (s, 2H), 3.90 (s, 2H) ppm. δ_C 197.0, 163.1, 161.1, 141.4, 137.8, 135.7, 130.0, 128.9, 128.8, 128.6, 128.3, 128.0, 118.4, 115.5, 115.3, 73.8, 69.8, 38.9 ppm. δ_F 62.3 ppm. MS (APPI): m/z 325 $[M + H]^+$.

1-(Benzyloxy)methyl-2-chloro-5-(formylmethyl)-4-phenylimidazole (15h). Preparation was done according to the general procedure from **14h** (1.6 g, 4.6 mmol) affording **15h** (1.0 g, 63%) as a yellow syrup, R_f = 0.50/(1:1 EtOAc/*n*-heptane). NMR ($CDCl_3$): δ_H 9.72 (t, J = 1.4, 1H), 7.52−7.49 (m, 2H), 7.41−7.29 (m, 8H), 5.35 (s, 2H), 4.52 (s, 2H), 3.94 (d, J = 1.4, 2H) ppm. δ_C 196.8, 141.0, 136.0, 132.9, 132.7, 128.6, 128.3, 127.9, 127.7, 127.6, 127.3, 120.5, 73.3, 70.6, 39.5 ppm. MS (APPI): m/z 341 $[M + H]^+$.

1-(Benzyloxy)methyl-5-(formylmethyl)-2-methyl-4-phenylimidazole (15i). Preparation was done according to the general procedure from **14i** (1.6 g, 4.7 mmol) affording **15i** (1.2 g, 77%) as a yellow oil, R_f = 0.38/EtOAc. NMR ($CDCl_3$): δ_H 9.66 (t, J = 1.4, 1H), 7.53−7.51 (m, 2H), 7.38−7.25 (m, 8H), 5.18 (s, 2H), 4.45 (s, 2H), 3.85 (d, J = 1.4, 2H), 2.41 (s, 3H) ppm. δ_C 197.6, 145.5, 139.8, 136.1, 134.0, 128.5, 128.4, 128.2, 127.6, 127.2, 127.0, 118.2, 72.4, 69.8, 39.3, 13.2 ppm. MS (APPI): m/z 321 $[M + H]^+$.

General Procedure for the $NaClO_2$ Oxidation of Compounds 12b−g and 15h,i. A solution of $NaClO_2$ (3 equiv) and $NaH_2PO_4 \cdot H_2O$ (5 equiv) in water (3.3 mL/mmol aldehyde) was added dropwise at 0 °C to a solution of the aldehyde and 2-methyl-2-butene (20 equiv) in CH_3CN (6.6 mL/mmol aldehyde). The resulting two-phase system was stirred vigorously for 90 min at room temperature followed by addition of 6 M HCl (aq) to pH 1. The resulting turbid solution was continuously extracted with EtOAc. The organic phase from the continuous extraction was evaporated in vacuo, and the crude product was purified by filtration through silica gel (most impurities were eluted with EtOAc, and the acid was eluted with MeOH). The purified acid was generally more than 95% pure according to LC/MS. The crude acid was dissolved in absolute EtOH (80 mL), and HCl/EtOH was added. The reaction mixture was heated to reflux for 30 min (1 h for the synthesis of **13b**, **13d**, and **13e**), cooled to room temperature, and evaporated in vacuo. The residue was suspended in saturated aqueous $NaHCO_3$ followed by extraction with EtOAc. The combined organic phases were washed with brine, dried ($MgSO_4$), and evaporated in vacuo. DCVC afforded the desired ethyl ester.

1-(Benzyloxy)methyl-5-(ethoxycarbonyl)methyl-4-iodoimidazole (13b). Preparation was done according to the general procedure from **12b** (0.62 g, 1.7 mmol) to give **13b** (0.29 g, 41%) as a colorless oil, R_f = 0.67/EtOAc. NMR ($CDCl_3$): δ_H 7.49 (s, 1H), 7.38−7.31 (m, 3H), 7.27−7.26 (m, 2H), 5.36 (s, 2H), 4.41 (s, 2H), 4.12 (q, J = 7.1, 2H), 3.72 (s, 2H), 1.24 (t, J = 7.1, 3H) ppm. δ_C 168.9, 139.5, 135.8, 128.7, 128.4, 128.0, 127.8, 87.8, 74.4, 70.0, 61.4, 30.9, 14.1 ppm. MS (APPI): m/z 401 $[M + H]^+$. Anal. ($C_{15}H_{17}N_2O_3I$) C, H, N.

1-(Benzyloxy)methyl-5-(ethoxycarbonyl)methyl-4-phenylimidazole (13c). Preparation was done according to the general procedure from **12c** (1.0 g, 3.3 mmol) to give **13c** (0.58 g, 50%) as a pale-yellow oil, R_f = 0.42/EtOAc. NMR ($CDCl_3$): δ_H 7.68−7.66 (m, 2H), 7.58 (s, 1H), 7.43−7.40 (m, 2H), 7.37−7.29 (m, 6H), 5.41 (s, 2H), 4.46 (s, 2H), 4.14 (q, J = 7.1, 2H), 3.88 (s, 2H), 1.24 (t, J = 7.1, 3H) ppm. δ_C 170.0, 141.6, 137.7, 136.1, 134.2, 128.6, 128.4, 128.2, 128.0, 127.4, 127.1, 120.3, 74.0, 69.8, 61.3, 30.2, 14.1 ppm. MS (APPI): m/z 351 $[M + H]^+$.

1-(Benzyloxy)methyl-5-(ethoxycarbonyl)methyl-4-(2-methylphenyl)imidazole (13d). Preparation was done according to the general procedure from **12d** (1.4 g, 4.4 mmol) to give **13d** (0.44 g, 27%) as a yellow oil, R_f = 0.45/EtOAc. NMR ($CDCl_3$): δ_H 7.58 (s, 1H), 7.36−7.16 (m, 9H), 5.37 (s, 2H), 4.45 (s, 2H), 4.04 (q, J = 7.3, 2H), 3.63 (s, 2H), 2.31 (s, 3H), 1.17 (t, J = 7.3, 3H) ppm. δ_C 169.8, 141.9, 137.7, 137.1, 136.1, 133.2, 130.2, 130.1, 128.4, 128.1, 127.8, 127.7, 125.2, 121.0, 74.1, 69.7, 60.9, 29.4, 19.9, 13.8 ppm. MS (APPI): m/z 365 $[M + H]^+$.

1-(Benzyloxy)methyl-5-(ethoxycarbonyl)methyl-4-(3-methylphenyl)imidazole (13e). Preparation was done according to the general procedure from **12e** (1.1 g, 3.3 mmol) to give **13e** (0.40 g, 33%) as an orange oil, R_f = 0.43/EtOAc. NMR ($CDCl_3$): δ_H 7.55 (s, 1H), 7.53 (br s, 1H), 7.45 (br d, J = 7.5, 1H), 7.34−7.25 (m, 6H), 7.11 (br d, J = 7.5, 1H), 5.37 (s, 2H), 4.41 (s, 2H), 4.12 (q, J = 7.1, 2H), 3.86 (s, 2H), 2.38 (s, 3H), 1.22 (t, J = 7.1, 3H) ppm. δ_C 169.8, 141.4, 137.8, 137.5, 136.0, 133.9, 128.3, 128.1, 127.97, 127.96, 127.7, 127.6, 124.1, 120.1, 73.9, 69.6, 61.1, 29.9, 21.2, 13.9 ppm. MS (APPI): m/z 365 $[M + H]^+$.

1-(Benzyloxy)methyl-5-(ethoxycarbonyl)methyl-4-(4-methylphenyl)imidazole (13f). Preparation was done according to the general procedure from **12f** (0.62 g, 2.0 mmol) to give **13f** (0.71 g, 69%) as a yellow oil, R_f = 0.49/EtOAc. NMR ($CDCl_3$): δ_H 7.58 (d, J = 8.2, 2H), 7.53 (s, 1H), 7.31−7.19 (m, 7H), 5.33 (s, 2H), 4.38 (s, 2H), 4.08 (q, J = 7.1, 2H), 3.83 (s, 2H), 2.33 (s, 3H), 1.18 (t, J = 7.1, 3H) ppm. δ_C 169.6, 141.2, 137.3, 136.3, 135.9, 131.1, 128.8, 128.2, 127.8, 127.6, 126.9, 119.6, 73.7, 69.4, 60.9, 29.8, 20.8, 13.7 ppm. MS (APPI): m/z 365 $[M + H]^+$.

1-(Benzyloxy)methyl-5-(ethoxycarbonyl)methyl-4-(4-fluorophenyl)imidazole (13g). Preparation was done according to the general procedure from **12g** (0.46 g, 1.4 mmol) to give **13g** (0.24 g, 45%) as a pale-yellow oil, R_f = 0.37/EtOAc. NMR ($CDCl_3$): δ_H 7.66−7.62 (m, 2H), 7.56 (s, 1H), 7.38−7.29 (m, 5H), 7.12−7.09 (m, 2H), 5.41 (s, 2H), 4.46 (s, 2H), 4.14 (q, J = 7.2, 2H), 3.84 (s, 2H), 1.24 (t, J = 7.2, 3H) ppm. δ_C 169.9, 163.2, 161.2, 140.9, 137.7, 136.1, 130.3, 129.1, 129.0, 128.6, 128.3, 128.0, 120.1, 115.5, 115.3, 74.1, 69.9, 61.4, 30.1, 14.1 ppm. δ_F 61.7 ppm. MS (APPI): m/z 369 $[M + H]^+$.

1-(Benzyloxy)methyl-2-chloro-5-(ethoxycarbonyl)methyl-4-phenylimidazole (16h). Preparation was done according to the general procedure from **15h** (0.53 g, 1.6 mmol) to give **16h** (43 mg, 7%) as a spectroscopically pure colorless oil and 2-chloro-

4(5)-(ethoxycarbonyl)methyl-5(4)-phenylimidazole (0.17 g, 41%). Analytical data for **16h**: R_f = 0.61/(1:1 EtOAc/*n*-heptane). NMR ($CDCl_3$): δ_H 7.62 (br d, J = 7.3, 2H), 7.40 (t, J = 7.8, 2H), 7.36−7.30 (m, 6H), 5.50 (s, 2H), 4.53 (s, 2H), 4.14 (q, J = 7.3, 2H), 3.86 (s, 2H), 1.24 (t, J = 7.3, 3H) ppm. δ_C 169.7, 140.3, 136.4, 133.2, 132.5, 128.6, 128.5, 128.2, 127.8, 127.5, 127.4, 122.3, 73.5, 70.6, 61.6, 30.6, 14.1 ppm. MS (APPI): *m*/*z* 385 $[M + H]^+$. Analytical data for 2-chloro-4(5)-(ethoxycarbonyl)methyl-5(4)-phenylimidazole: Colorless oil, R_f = 0.38/(1:1 EtOAc/*n*-heptane). NMR ($CDCl_3$): δ_H 12.8 (br s, 1H), 7.44 (d, J = 7.1, 2H), 7.31 (dd, J = 7.1, J = 7.8, 2H), 7.25 (d, J = 7.3, 1H), 4.10 (q, J = 7.1, 2H), 3.68 (s, 2H), 1.17 (t, J = 7.1, 3H) ppm. δ_C 170.7, 130.9, 130.6, 128.6, 127.4, 127.1, 61.2, 32.4, 13.9 ppm. MS (APPI): *m*/*z* 265 $[M + H]^+$. Anal. ($C_{13}H_{13}N_2O_2Cl$) C, H, N.

1-(Benzyloxy)methyl-5-(ethoxycarbonyl)methyl-2-methyl-4-phenylimidazole (16i). Preparation was done according to the general procedure from **15i** (1.1 g, 3.5 mmol) to give **16i** (0.62 g, 49%) as an orange oil, R_f = 0.43/EtOAc. NMR ($CDCl_3$): δ_H 7.65−7.63 (m, 2H), 7.40−6.75 (m, 8H), 5.34 (s, 2H), 4.47 (s, 2H), 4.12 (q, J = 7.3, 2H), 3.80 (s, 2H), 2.43 (s, 3H), 1.22 (t, J = 7.3, 3H) ppm. δ_C 170.1, 145.2, 139.0, 136.3, 134.2, 128.4, 128.2, 128.0, 127.5, 127.3, 126.7, 120.0, 72.6, 69.7, 61.1, 30.3, 13.9, 13.3 ppm. MS (APPI): *m*/*z* 365 $[M + H]^+$.

General Procedure for Deprotection of 13b−g and 16h,i. The ethyl ester was suspended in 48% HBr (aq) (50 equiv). This mixture was heated to 110 °C for 1 h, cooled to room temperature, and evaporated in vacuo. The residue was dissolved in water, filtered through cotton, and coevaporated in vacuo. Additional coevaporations from water provided the crude hydrobromide.

4(5)-(Carboxymethyl)-5(4)-iodoimidazole Trifluoroacetate (8b). Preparation was done according to the general procedure. The crude product (0.18 g) obtained from **13b** (0.22 g, 0.55 mmol) was dissolved in a minimum of MeOH and precipitated with EtO_2 to afford **8b** as the hydrobromide salt (0.11 g, 81%). MS (APPI): *m*/*z* 253 $[M + H]^+$. (**8b** was contaminated with a small amount of IAA (**4**) (191:9) judged by ^1H NMR and HPLC analyses.) An analytical amount was purified by RPC [(H_2O)−(0.1% TFA)−(0 → 6% CH_3CN), with increments of 3%] to give the product as light-brown crystals (25 mg): mp 125−130 °C. NMR (D_2O): δ_H 8.73 (s, 1H), 3.80 (s, 2H) ppm. δ_C 173.1, 136.6, 131.5, 70.6, 31.7 ppm. Anal. ($C_5H_5N_2O_2I \cdot C_2HF_3O_2$) C, H, N.

4(5)-(Carboxymethyl)-5(4)-phenylimidazole Hydrobromide (8c). Preparation was done according to the general procedure. The crude product obtained from **13c** (0.20 g, 0.57 mmol) was dissolved in a minimum of MeOH and precipitated with EtO_2 to afford **8c** (0.11 g, 71%) as colorless needles: mp >250 °C. NMR (CD_3OD): δ_H 8.99 (s, 1H), 7.57−7.52 (m, 5H), 4.88 (br s, 2H), 3.89 (s. 2H) ppm. δ_C 171.9, 134.7, 132.2, 131.1, 130.6, 129.2, 127.9, 124.4, 30.8 ppm. MS (APPI): *m*/*z* 203 $[M - HBr]^+$. Anal. ($C_{11}H_{10}N_2O_2 \cdot HBr$) C, H, N.

4(5)-(Carboxymethyl)-5(4)-(2-methylphenyl)imidazole Trifluoroacetate (8d). Preparation was done according to the general procedure from **13d** (0.17 g, 0.47 mmol) to give the hydrobromide of **8d** (0.10 g, 68%). MS (APPI): *m*/*z* 217. Part of the hydrobromide **8d** was purified by RPC [(H_2O)−(0.1% TFA)−(0 → 15% CH_3CN), with increments of 5%] to give the product as colorless crystals (28 mg): mp 100−103 °C. NMR (D_2O): δ_H 8.66 (s, 1H), 7.43−7.32 (m, 2H), 7.30−7.21 (m, 2H), 3.56 (s, 2H), 2.15 (s, 3H) ppm. δ_C 174.6, 138.6, 132.6, 130.9, 130.9, 130.7, 129.5, 126.4, 125.6, 124.7, 30.9, 19.1 ppm. Anal. ($C_{12}H_{12}N_2O_2 \cdot 0.6C_2HF_3O_2$) C, H, N.

4(5)-(Carboxymethyl)-5(4)-(3-methylphenyl)imidazole Hydrobromide (8e). Preparation was done according to the general procedure. The crude product (0.12 g, 56%) obtained from **13e** (0.23 g, 0.64 mmol) was pure according to NMR: mp 70−72 °C. NMR (CD_3OD): δ_H 8.99 (s, 1H), 7.44 (t, 1H, J = 7.5 Hz), 7.38 (br s, 1H), 7.34 (br d, 2H, J = 7.3 Hz), 4.91 (br s, 2H), 3.88 (s, 2H), 2.42 (s, 3H) ppm. δ_C 171.9, 140.7, 134.6, 132.3, 131.7, 130.5, 129.6, 127.8, 126.2, 124.2, 30.9, 21.5 ppm. MS (APPI): *m*/*z* 217. Anal. ($C_{12}H_{12}N_2O_2 \cdot HBr \cdot H_2O$) C, H. N found 8.39, N calcd 8.89.

4(5)-(Carboxymethyl)-5(4)-(4-methylphenyl)imidazole Hydrobromide (8f). Preparation was done according to the general procedure. The crude product obtained from **13f** (0.35 g, 0.96 mmol) was dissolved in a minimum of MeOH and precipitated with Et_2O to afford **8f** (0.24 g, 83%) as a light-brown solid: mp >250 °C. NMR (CD_3OD): δ_H 8.96 (s, 1H), 7.45 (d, J = 8.0, 2H), 7.39 (d, J = 8.0, 2H), 4.86 (br s, 2H), 3.87 (s, 2H), 2.42 (s, 3H) ppm. δ_C 171.9, 141.6, 134.5, 132.3, 131.2, 129.1, 125.0, 124.0, 30.8, 21.4 ppm. MS (APPI): *m*/*z* 217 $[M - HBr]^+$. Anal. ($C_{12}H_{12}N_2O_2 \cdot HBr \cdot 0.25H_2O$) C, H, N.

4(5)-(Carboxymethyl)-5(4)-(4-fluorophenyl)imidazole Hydrobromide (8g). Preparation was done according to the general procedure. The crude product obtained from **13g** (0.11 g, 0.30 mmol) was partially dissolved in acetone and precipitated with *n*-heptane to afford **8g** (55 mg, 61%) as a light-brown solid: mp 202 °C (dec). NMR (CD_3OD): δ_H 8.98 (s, 1H), 7.63−7.60 (m, 2H), 7.34−7.30 (m, 2H), 4.90 (br s, 2H), 3.87 (s, 2H) ppm. δ_C 171.8, 166.0, 164.1, 134.7, 131.7, 131.6, 131.3, 124.5, 124.2, 124.2, 117.6, 117.5, 30.7 ppm. δ_F −113 ppm. MS (APPI): *m*/*z* 221 $[M - HBr]^+$. Anal. ($C_{11}H_9N_2O_2F \cdot HBr \cdot 0.25H_2O$) C, H, N.

4(5)-(Carboxymethyl)-2-chloro-5(4)-phenylimidazole Hydrobromide (8h). Preparation was done according to the general procedure. The crude product obtained from **16h** (0.14 g, 0.52 mmol) was dissolved in a minimum of MeOH and precipitated with Et_2O to afford **8h** (0.13 g, 78%) as colorless crystals: mp 201 °C (dec). NMR (CD_3OD): δ_H 7.59−7.52 (m, 5H), 4.92 (br s, 2H), 3.84 (s, 2H) ppm. δ_C 171.7, 133.8, 131.2, 130.6, 129.2, 129.1, 127.7, 125.8, 31.1 ppm. MS (APPI): *m*/*z* 237 $[M - HBr]^+$. Anal. ($C_{11}H_9N_2O_2Cl \cdot HBr \cdot 0.25H_2O$) C, H, N.

4(5)-(Carboxymethyl)-2-methyl-5(4)-phenylimidazole Hydrobromide (8i). Preparation was done according to the general procedure. The crude product from **16i** (0.21 g, 0.57 mmol) afforded **8i** (0.11 g, 61%) as gray crystals: mp 110 °C (dec). NMR (CD_3OD): δ_H 7.58−7.49 (m, 5H), 4.87 (br s, 2H), 3.83 (s, 2H), 2.68 (s, 3H) ppm. δ_C 172.0, 131.4, 130.8, 130.5, 128.9, 128.9, 128.2, 123.4, 30.9, 11.4 ppm. MS (APPI): *m*/*z* 217 $[M - HBr]^+$. Anal. ($C_{12}H_{12}N_2O_2 \cdot HBr \cdot 1.5H_2O$) C, H, N.

2-Methyl-1-(*N*,*N*-dimethylsulfamoyl)imidazole (17).[35] *N*,*N*-Dimethylsulfamoyl chloride (13.0 mL, 121 mmol) and Et_3N (70 mmol) were added to a solution of 2-methylimidazole (61 mmol) in 1,2-dichloroethane (70 mL), and this mixture was stirred at room temperature for 20 h. After filtration and wash of the filter cake with 1,2-dichloroethane, the combined filtrate and wash were washed with saturated aqueous Na_2CO_3, dried, and evaporated in vacuo. Distillation (92−95 °C, 0.5 mmHg) afforded the title compound (10.3 g, 90%) as a colorless oil. NMR ($CDCl_3$): δ_H 7.22 (d, J = 1.4, 1H), 6.92 (d, J = 1.4, 1H), 2.90 (s 6H), 2.61 (s, 3H) ppm. δ_C 146.2, 127.4, 120.1, 38.7, 15.8 ppm.

4(5)-Formyl-2-methylimidazole (18).[68] A solution of **17** (5.5 g, 29 mmol) in dry THF (200 mL) was cooled to −78 °C. *n*-BuLi (20 mL, 1.6 M in hexane, 35 mmol) was added keeping the temperature below −76 °C. After the mixture was stirred at −78 °C for 30 min, DMF (14 mL, 182 mmol) was added followed by stirring at −78 °C for 1 h. The reaction mixture was heated to room temperature over 1 h and stirred at room temperature for 30 min. The pH was adjusted to 1 with concentrated HCl (aq), and the resulting mixture was stirred for 2 h. The pH was then adjusted to 8 with saturated aqueous $NaHCO_3$, and THF was evaporated in vacuo. The residue was extracted with EtOAc (3 × 150 mL). The combined organic phases was dried ($MgSO_4$) and evaporated in vacuo to afford the title compound (2.6 g, 82%) as faint yellow crystals. NMR (DMSO-d_6): δ_H 12.74 (br s, 1H), 9.61 (s, 1H), 7.84 (br s, 1H), 2.33 (s, 3H) ppm. δ_C 184.9, 179.1, 151.5, 147.1, 141.6, 132.8, 126.7, 14.2 ppm. Anal. ($C_5H_6N_2O$) C, H, N.

4(5)-(Hydroxymethyl)-2-methylimidazole (19j).[37] $NaBH_4$ (92 mg, 2.43 mmol) was added to a solution of **18** (0.27 g, 2.43 mmol) in ethanol (12 mL). This mixture was stirred for 3 h, after which brine (5 mL) was added. The resulting mixture was extracted three times with EtOAc, and the combined organic phases were dried ($MgSO_4$). Evaporation in vacuo provided the title compound (0.26 g, 95%) as colorless crystals, which was used without further purification. NMR (DMSO-d_6): δ_H 6.71 (s, 1H), 4.30 (s, 2H), 2.23 (s, 3H) ppm. δ_C 143.6, 137.0, 117.7, 56.3, 14.0 ppm.

4(5)-(Chloromethyl)-2-methylimidazole Hydrochloride (20j).[37] **19j** (0.46 g, 4.1 mmol) was dissolved in $SOCl_2$ (1.2 g, 10.3 mmol) and stirred at room temperature for 4 h. $CHCl_3$ (6 mL) was added followed by evaporation in vacuo to provide **20j** (0,64 g, 93%) as yellow crystals, which were used without further purification. NMR (DMSO-d_6): δ_H 7.59 (s, 1H), 4.84 (s, 2H), 2.58 (s, 3H) ppm. δ_C 145.6, 128.8, 118.0, 54.2, 11.5 ppm.

4(5)-(Hydroxymethyl)-2-phenylimidazole (19k).[36] A suspension of benzamidine hydrochloride (3.13 g, 20 mmol), dihydroxyacetone dimer (3.68 g, 41 mmol), and NH_4Cl (4.4 g) in NH_4OH (30 mL) was heated at 80 °C for 30 min. The cooled reaction mixture was extracted with EtOAc (6 × 100 mL), dried ($MgSO_4$), and evaporated in vacuo to give **19k** (2.67 g, 77%) as colorless crystals. NMR (DMSO-d_6): δ_H 7.93 (d, J = 8.0, 2H), 7.42 (t, J = 8.0, 2H), 7.32 (t, J = 8.0, 1H), 7.00 (s, 1H), 4.44 (s, 2H) ppm. δ_C 143.9, 129.7, 129.0, 127.4, 126.5, 123.6, 123.4, 36.1 ppm.

4(5)-(Chloromethyl)-2-phenylimidazole hydrochloride (20k).[36] **19k** (0.55 g, 3.1 mmol) was dissolved in $SOCl_2$ (0.74 g, 6.2 mmol) and stirred for 90 min at 80 °C, after which the reaction mixture was cooled to room temperature and evaporated in vacuo. The residue was dissolved in $CHCl_3$ (4 mL), and the resulting solution was evaporated in vacuo. Additional coevaporations with $CHCl_3$ gave **20k** (0.67 g, 93%) as brown crystals, which were used without further purification. NMR (DMSO-d_6): δ_H 8.23−8.13 (m, 2H), 7.84 (s, 1H), 7.64 (t, J = 3.3, 3H), 4.93 (s, 2H) ppm. δ_C 144.6, 132.5, 131.0, 129.8, 127.3, 123.5, 119.9, 35.0 ppm.

4(5)-(Cyanomethyl)-2-methylimidazole (21j).[37] **20j** (0.28 g, 1.7 mmol) was added to a solution of NaCN (0.41 g, 8.4 mmol) in DMSO (10 mL), and the resulting solution was stirred at room temperature for 24 h. Saturated aqueous $NaHCO_3$ (5 mL) was added (pH 8) followed by continuous extraction with EtOAc. The organic phase was dried ($MgSO_4$) and evaporated in vacuo. The residue was washed with Et_2O and treated with activated carbon to afford **19j** (0.11 g, 56%) as pale-yellow crystals, which were used without further purification. NMR (DMSO-d_6): δ_H 11.66 (br s, 1H), 6.88 (s, 1H), 3.72 (s, 2H), 2.23 (s, 3H) ppm. δ_C 144.2, 129.5, 119.2, 114.0, 16.7, 14.1 ppm.

4(5)-(Cyanomethyl)-2-phenylimidazole (21k).[36] A solution of **20k** (0.67 g, 2.9 mmol) in DMSO (8 mL) was added to a solution of NaCN (0.72 g, 14.6 mmol) in DMSO (10 mL), and this reaction mixture was stirred at room temperature for 5 h. Saturated aqueous $NaHCO_3$ (5 mL) was added (pH 8), and this mixture was extracted with EtOAc. The organic phase was dried ($MgSO_4$) and evaporated in vacuo to afford **19k** (0.33 g, 62%) as brown crystals, which were used without further purification. NMR (DMSO-d_6): δ_H 12.55 (br s, 1H), 7.91 (d, J = 7.0, 2H), 7.45 (t, J = 7.0, 2H), 7.35 (t, J = 7.0, 1H), 7.20 (s, 1H), 3.90 (s, 2H) ppm. δ_C 146.2, 132.0, 130.6, 129.1, 128.6, 125.2, 119.3, 115.8, 17.1 ppm.

4(5)-(Carboxymethyl)-5(4)-methylimidazole Hydrochloride (8a).[36] 4(5)-(Cyanomethyl)-5(4)-methylimidazole (**21a**) for use in this reaction was obtained from **19a** via **20a** as described by Rosen et al.[34] A solution of **21a** (0.30 g, 2.5 mmol) in 48% aqueous HBr (15 mL) was boiled under reflux for 90 min and then evaporated in vacuo. The residue was dissolved in HCl/EtOH (15 mL), and this solution was boiled under reflux for 2.5 h followed by evaporation in vacuo. EtOAc (30 mL) and saturated aqueous $NaHCO_3$ (6 mL) were added. After two extractions with EtOAc the combined organic phases were dried ($MgSO_4$) and evaporated in vacuo. The residue obtained was dissolved in concentrated HCl (aq) (15 mL) and stirred for 5 h at 50 °C followed by evaporation in vacuo. The residue was suspended in boiling acetonitrile. Filtration and drying in vacuo afforded **8a** (291 mg, 66%) as colorless crystals: mp 203.5−204.9 °C. NMR (DMSO-d_6): δ_H 8.90 (s, 1H), 3.73 (s, 2H), 2.22 (s, 3H) ppm. δ_C 170.6, 132.4, 126.6, 122.7, 29.3, 8.8 ppm. Anal. ($C_6H_8N_2O_2$·HCl) C, H, N.

4(5)-(Carboxymethyl)-2-methylimidazole Hydrochloride (8j).[36] Preparation was done as described for **8a** from **21j** (275 mg, 2.27 mmol) affording **8j** (169 mg, 42%) as colorless crystals: mp 172.2−173.7 °C. NMR (DMSO-d_6): δ_H 7.34 (s, 1H), 3.73 (s, 2H), 2.54 (s, 3H) ppm. δ_C 170.6, 144.4, 126.3, 116.9, 30.4, 11.4 ppm. Anal. ($C_6H_8N_2O_2$·HCl·0.5H_2O) C, H, N.

4(5)-(Carboxymethyl)-2-phenylimidazole Hydrochloride (8k).[36] Preparation was done as described for **8a** from **21k** (0.53 g, 2.9 mmol). The residue was dissolved in concentrated HCl (aq) (5 mL) and stirred at 50 °C for 24 h to provide a suspension. The product was filtered off, washed, and dried in vacuo to afford **8k** (0.23 g, 43%) as colorless crystals: mp 202.2−203.5 °C. NMR (DMSO-d_6): δ_H 8.18−8.08 (m, 2H), 7.68−7.62 (m, 3H), 7.61 (s, 1H), 3.86 (s, 2H) ppm. δ_C 170.5, 143.3, 132.2, 129.9, 128.5, 126.9, 123.5, 118.8, 30.6 ppm. Anal. ($C_{11}H_{10}N_2O_2$·HCl·H_2O) C, H, N.

1-(Benzyloxy)-2-chloro-5-(cyanomethyl)imidazole (23). A suspension of **22**[38] (2.0 g, 6.8 mmol) in DMF (15 mL) was added to a solution of KCN (2.5 g, 39 mmol) in H_2O (2 mL), and the reaction mixture was stirred for 24 h at room temperature. Saturated aqueous $NaHCO_3$ (5 mL) was added (pH 8) followed by two extractions with EtOAc. The combined organic phases were dried ($MgSO_4$) and evaporated in vacuo. The resulting brown oil was subjected to CC (*n*-heptane/EtOAc 100:0 → 60:40) to provide **23** (0.99 g, 59%) as a brown oil. NMR (DMSO-d_6): δ_H 7.55−7.51 (m, 2H), 7.50−7.44 (m, 3H), 6.86 (s, 1H), 5.30 (s, 2H), 4.09 (s, 2H) ppm. δ_C 130.7, 128.3, 127.8, 126.8, 125.1, 120.7, 119.5, 114.6, 79.4, 10.6 ppm. Anal. ($C_{12}H_{10}N_3OCl$) C, H, N.

4(5)-(Carboxymethyl)-2-chloroimidazole Hydrochloride (8l). Preparation was done via 5-(carboxymethyl)-2-chloro-1-hydroxyimidazole hydrochloride (24), which was prepared as described for **8a** from **23** (0.89 g, 3.6 mmol) to give the 1-hydroxyimidazole (0.44 g, 58%) as pale-yellow crystals. NMR (DMSO-d_6): δ_H 6.85 (s, 1H), 3.63 (s, 2H) ppm. δ_C 170.5, 126.4, 126.1, 121.3, 29.5 ppm. A solution of **24** (0.20 g, 0.95 mmol) in methanol (6 mL) was cooled to 0 °C followed by dropwise addition of $TiCl_3$ (10% in 20% aqueous HCl, 2.6 mL, 1.7 mmol). The reaction mixture was stirred at 0 °C for 3 h, heated to room temperature, and stirred 1 h at room temperature. The pH was adjusted to 8 with saturated aqueous $NaHCO_3$, and the resulting mixture was extracted three times with EtOAc. The combined organic phases were dried ($MgSO_4$) and evaporated in vacuo. The residue was dissolved in concentrated HCl (aq) (5 mL) and stirred for 4 h at 50 °C. Evaporation in vacuo afforded **8l** (0.12 g, 63%) as colorless crystals: mp 194 °C (dec). NMR (DMSO-d_6): δ_H 11.45 (br s, 1H), 7.15 (s, 1H), 3.58 (s, 2H) ppm. δ_C 171.2, 130.6, 128.6, 119.8, 32.1 ppm. Anal. ($C_5H_5N_2O_2Cl$·HCl) H. C found 31.08, C calcd 30.48. N found 13.65, N calcd 14.22.

Pharmacology. Materials. Culture media, serum, antibiotics, and buffers for cell culture were obtained from Invitrogen (Paisley, U.K.). GABA was obtained from Sigma, and TPMPA was purchased from Tocris Cookson (U.K.). The compounds muscimol, THIP, and isoguvacine were synthesized in the lab. The cDNA for the human ρ1 subunit (hρ1-pcDNA3.1) was a kind gift from Dr. David S. Weiss (University of Alabama, AL).

[^{3}H]Muscimol Binding to Rat Brain Tissue. The affinities toward $GABA_A$ receptors was determined in rat brain membrane preparations using [^{3}H]muscimol as the radioligand and performed as described previously.[25]

Molecular Biology. The Ser168Thr mutation in human ρ1-pcDNA3.1 and the Thr129Ser mutation in rat α_1-pCis were made using the QuickChange mutagenesis kit according to the manufacturer's instructions (Stratagene, La Jolla, CA). The absence of unwanted mutations was verified by sequencing the cDNAs.

Generation of the Stable hρ_1-HEK293 Cell Line. The stable hρ1-HEK293 cell line was constructed essentially as previously described for stable cell lines of glycine receptors.[61,69] Briefly, HEK 293 cells were maintained at 37 °C in a humidified 5% CO_2 incubator in culture medium [Dulbecco's modified Eagle medium (DMEM) supplemented with penicillin (100 U/mL), streptomycin (100 μg/mL), and 10% dialyzed fetal bovine serum]. The cells were transfected with hρ1-pcDNA3.1 using Polyfect as a DNA carrier according to the protocol by the manufacturer (Qiagen, Hilden, Germany). The transfected cells were maintained for 2−3 weeks in culture medium containing 3 mg/mL G-418. G418-resistant colonies were isolated and maintained in culture medium supplemented with 1 mg/mL G-418 and for 2−3 weeks. Cell colonies were screened for a functional response to 100 μM GABA in the

FLIPR membrane potential (FMP) assay (see below). On the basis of this screening, where several cell clones exhibiting a significant response to GABA exposure were identified, one single clone was selected for further characterization.

Transient Transfections. The HEK 293 cells (ECACC, U.K.) used for the patch-clamp experiments were maintained at 37 °C in a humidified 5% CO_2 incubator in culture medium [Dulbecco's modified Eagle medium (DMEM) supplemented with penicillin (100 U/mL), streptomycin (100 μg/mL), and 10% dialyzed fetal bovine serum]. Before transfection the cells were split into 35 mm Petri dishes. After 18−24 h, the cells were transfected with a combination of rat α_1-pCis, β_2-pCis, and γ_{2S}-pCis (1:1:2 ratio), with rat α_1(Thr129Ser)-pCis, β_2-pCis, and γ_{2S}-pCis (1:1:2 ratio), or with human ρ_1-pcDNA3.1 and cotransfected with plasmid coding for green fluorescent protein (pGreen Lantern, Life technologies, Paisley, U.K.) in order to visualize transfected cells. Targefect F1 was used as a DNA carrier in DMEM without serum according to the manufacturer's protocol (Targeting Systems, CA) and used for the patch-clamp experiments 20−72 h after transfection.

In the experiments using transiently transfected tsA-201 cells, the tsA-201 cells (a transformed HEK293 cell line) were maintained at 37 °C in a humidified 5% CO_2 incubator in DMEM supplemented with penicillin (100 U/mL), streptomycin (100 μg/mL), and 10% dialyzed fetal bovine serum. The cells were split into 10 cm tissue culture dishes, and the following day they were transfected with WT and Ser168Thr hρ1-pcDNA3.1 using Polyfect as a DNA carrier. After 16−24 h, the cells were split into poly-D-lysine-coated black 96-well plates (Packard) and used the following day for the FMP assay.

FLIPR Membrane Potential (FMP) Assay. The stable hρ1-HEK293 cell line and tsA-201 cells transiently transfected with WT or S168T hρ1-pCDNA3.1 were characterized pharmacologically in the FMP assay according to the protocol of the manufacturer (Molecular Devices). The cells were split into poly-D-lysine-coated black 96-well plates (Packard) in culture medium (in the case of the stable cell line, the medium was supplemented with 1 mg/mL G-418). After 16−24 h, the medium was aspirated, and the cells were washed with 100 μL of assay buffer [Hanks buffered saline solution supplemented with 20 mM HEPES, pH 7.4]. 100 μL of assay buffer containing loading dye was added to each well (in the antagonist experiments, various concentrations of the antagonists were dissolved in the buffer), and the plate was incubated at 37 °C in a humidified 5% CO_2 incubator for 30 min. The plate was assayed in a NOVOstar plate reader (BMG Labtechnologies) measuring emission [in fluorescence units (FU)] at 560 nm caused by excitation at 530 nm before and up to 1 min after addition of 25 μL of agonist solution. The experiments were performed in duplicate at least three times for each compound.

Concentration−response curves for agonists and antagonists in the FMP assay were constructed on the basis of the maximal responses at different concentrations of the respective ligands. The curves were generated by nonweighted least-squares fits using the program KaleidaGraph 3.6 (Synergy Software). Antagonist potencies were calculated from the inhibition curves using the "functional equivalent" of the Cheng−Prusoff equation $K_i = IC_{50}/[1 + ([A]/EC_{50})]$,[70] where [A] is the agonist concentration used in the specific experiment.

Whole-Cell Patch-Clamp Experiments. Petri dishes with transfected cells were transferred to the stage of an Axiovert 10 microscope (Zeiss, Germany), and the culture medium was exchanged for extracellular recording solution at room temperature (20−22 °C). The extracellular solution contained the following (in mM): NaCl 140, KCl 3.5, Na_2HPO_4 1.25, $MgSO_4$ 2, $CaCl_2$ 2, glucose 10, and HEPES 10; pH 7.35. The cells were viewed at 200× magnification, and cells containing green fluorescent protein were visualized with UV light from a HBO 50 lamp (Zeiss, Germany). The cells were approached with micropipettes of 1.7−3 MΩ resistance manufactured from 1.5 mm OD glass (World Precision Instruments, Sarasota, FL). The intrapipette solution contained the following (in mM): KCl 140, $MgCl_2$ 1, $CaCl_2$ 1, EGTA 10, MgATP 2, and HEPES 10; pH 7.3. Standard patch-clamp techniques[71] in voltage clamp mode were used to record from neurons in the whole-cell configuration using an EPC-9 amplifier (HEKA, Germany). A clamping potential of −60 mV was usually used. Series resistance was 65−80% compensated. Whole-cell currents were recorded on a computer hard disk and on videotape using a VR-10 data recorder (Instrutech, NY) and analyzed subsequently using Pulse software (HEKA, Germany).

Extracellular solution containing the agonists was applied using a gravity-fed seven-barrelled perfusion pipet (List, Germany) ending approximately 100 μm from the recorded neuron. When the application was switched from one barrel to another, the extracellular solution surrounding the neuron was exchanged with a time constant of ∼50 ms.

For the $\alpha_1\beta_2\gamma_{2S}$ and the α_1(Thr129Ser)$\beta_2\gamma_{2S}$ receptors the agonists were applied for 5 s every 1 min. For the ρ_1 receptors, agonists were applied for 2−5 s every 30 s, except for GABA, which was applied for 2−5 s every 1−2 min. Between these drug applications, drug-free ABSS was applied from one of the barrels in order to quickly remove the drugs from the cell. For the agonist concentration-response relationship, the equation

$$I = \frac{I_{max}}{1 + \text{antilog}[(\log EC_{50} - A)n_H]}$$

was fitted to the experimental data, where I is the membrane current, A is the logarithm of the agonist concentration, I_{max} is the maximum current that the agonist can induce, EC_{50} is the agonist concentration eliciting 50% of I_{max}, and n_H is the Hill coefficient. Data were described using mean and standard error (SE) or 95% confidence intervals.

In some experiments with ρ_1 receptors, where current fade was observed during application of high agonist concentrations at the normal clamping potential of −60 mV, it was desirable to test whether this fade was due to desensitization or to shift of the Cl^- concentration gradient. For this purpose, the clamping potential was stepped between −40 and +40 mV at 0.5 s intervals for the duration of the agonist response in order to avoid a net shift of the Cl^- gradient. This procedure always abolished current fade, leaving no sign of desensitization of ρ_1 receptors.

Molecular Modeling. The model of the extracellular domain of the $\alpha_1\beta_2\gamma_2$ $GABA_A$ receptor was downloaded from http://www.univie.ac.at/brainresearch. Alternative conformations of amino acid residues in the binding pockets have been explored by the manual rotamer option in Insight II 2000 (Accelrys Software Inc.). Only low-energy conformations of the residues with respect to nonbonded interactions have been considered in the final ligand−receptor models.

Acknowledgment. The authors thank Dr. Weiss for his generous gift of the human ρ1 cDNA. The Danish Medicinal research Council supported this work. A.A.J. was supported by The Lundbeck Foundation. Ulla Geneser is thanked for technical assistance.

Supporting Information Available: Data from microanalysis. This material is available free of charge via the Internet at http://pubs.acs.org.

References

(1) Corringer, P. J.; Le Novere, N.; Changeux, J. P. Nicotinic receptors at the amino acid level. *Annu. Rev. Pharmacol. Toxicol.* **2000**, *40*, 431−458.

(2) Johnston, G. A. R. $GABA_A$ receptor channel pharmacology. *Curr. Pharm. Des.* **2005**, *11*, 1867−1885.

(3) Barnard, E. A.; Skolnick, P.; Olsen, R. W.; Mohler, H.; Sieghart, W.; Biggio, G.; Braestrup, C.; Bateson, A. N.; Langer, S. Z. International Union of Pharmacology. XV. Subtypes of gamma-aminobutyric $acid_A$ receptors: classification on the basis of subunit structure and receptor function. *Pharmacol. Rev.* **1998**, *50*, 291−313.

(4) Korpi, E. R.; Sinkkonen, S. T. GABA(A) receptor subtypes as targets for neuropsychiatric drug development. *Pharmacol. Ther.* **2006**, *109*, 12−32.

(5) Zhang, D.; Pan, Z. H.; Awobuluyi, M.; Lipton, S. A. Structure and function of GABA(C) receptors: a comparison of native versus recombinant receptors. *Trends Pharmacol. Sci.* **2001**, *22*, 121−132.

(6) Johnston, G. A.; Chebib, M.; Hanrahan, J. R.; Mewett, K. N. GABA-(C) receptors as drug targets. *Curr. Drug Targets: CNS Neurol. Disord.* **2003**, *2*, 260−268.

(7) Arnaud, C.; Gauthier, P.; Gottesmann, C. Study of a GABAC receptor antagonist on sleep-waking behavior in rats. *Psychopharmacology (Berlin)* **2001**, *154*, 415−419.

(8) McKernan, R. M.; Whiting, P. J. Which GABAA-receptor subtypes really occur in the brain? *Trends Neurosci.* **1996**, *19*, 139−143.

(9) Sieghart, W.; Sperk, G. Subunit composition, distribution and function of GABA(A) receptor subtypes. *Curr. Top. Med. Chem.* **2002**, *2*, 795−816.

(10) Ogurusu, T.; Yanagi, K.; Watanabe, M.; Fukaya, M.; Shingai, R. Localization of GABA receptor rho 2 and rho 3 subunits in rat brain and functional expression of homooligomeric rho 3 receptors and heterooligomeric rho 2 rho 3 receptors. *Recept. Channels* **1999**, *6*, 463−475.

(11) Enz, R.; Cutting, G. R. Molecular composition of GABAC receptors. *Vision Res.* **1998**, *38*, 1431−1441.

(12) Pan, Y.; Qian, H. Interactions between rho and gamma2 subunits of the GABA receptor. *J. Neurochem.* **2005**, *94*, 482−490.

(13) Ebert, B.; Thompson, S. A.; Suonatsou, K.; McKernan, R.; Krogsgaard-Larsen, P.; Wafford, K. A. Differences in agonist/antagonist binding affinity and receptor transduction using recombinant human gamma-aminobutyric acid type A receptors. *Mol. Pharmacol.* **1997**, *52*, 1150−1156.

(14) Vien, J.; Duke, R. K.; Mewett, K. N.; Johnston, G. A.; Shingai, R.; Chebib, M. *trans*-4-Amino-2-methylbut-2-enoic acid (2-MeTACA) and (+/−)-trans-2-aminomethylcyclopropanecarboxylic acid ((+/−)-TAMP) can differentiate rat rho3 from human rho1 and rho2 recombinant GABA(C) receptors. *Br. J. Pharmacol.* **2002**, *135*, 883−890.

(15) Woodward, R. M.; Polenzani, L.; Miledi, R. Characterization of bicuculline/baclofen-insensitive (rho-like) gamma-aminobutyric acid receptors expressed in Xenopus oocytes. II. Pharmacology of gamma-aminobutyric acidA and gamma-aminobutyric acidB receptor agonists and antagonists. *Mol. Pharmacol.* **1993**, *43*, 609−625.

(16) Kusama, T.; Spivak, C. E.; Whiting, P.; Dawson, V. L.; Schaeffer, J. C.; Uhl, G. R. Pharmacology of GABA rho 1 and GABA alpha/beta receptors expressed in Xenopus oocytes and COS cells. *Br. J. Pharmacol.* **1993**, *109*, 200−206.

(17) Ragozzino, D.; Woodward, R. M.; Murata, Y.; Eusebi, F.; Overman, L. E.; Miledi, R. Design and in vitro pharmacology of a selective gamma-aminobutyric acidC receptor antagonist. *Mol. Pharmacol.* **1996**, *50*, 1024−1030.

(18) Hansen, S. B.; Sulzenbacher, G.; Huxford, T.; Marchot, P.; Taylor, P.; Bourne, Y. Structures of Aplysia AChBP complexes with nicotinic agonists and antagonists reveal distinctive binding interfaces and conformations. *EMBO J.* **2005**, *24*, 3635−3646.

(19) Celie, P. H.; Kasheverov, I. E.; Mordvintsev, D. Y.; Hogg, R. C.; van Nierop, P.; van Elk, R.; van Rossum-Fikkert, S. E.; Zhmak, M. N.; Bertrand, D.; Tsetlin, V.; Sixma, T. K.; Smit, A. B. Crystal structure of nicotinic acetylcholine receptor homolog AChBP in complex with an alpha-conotoxin PnIA variant. *Nat. Struct. Mol. Biol.* **2005**, *12*, 582−588.

(20) Brejc, K.; van Dijk, W. J.; Klaassen, R. V.; Schuurmans, M.; van Der, Oost, J.; Smit, A. B.; Sixma, T. K. Crystal structure of an ACh-binding protein reveals the ligand-binding domain of nicotinic receptors. *Nature* **2001**, *411*, 269−276.

(21) Ernst, M.; Brauchart, D.; Boresch, S.; Sieghart, W. Comparative modeling of GABA(A) receptors: limits, insights, future developments. *Neuroscience* **2003**, *119*, 933−943.

(22) Sedelnikova, A.; Smith, C. D.; Zakharkin, S. O.; Davis, D.; Weiss, D. S.; Chang, Y. Mapping the ρ1 GABA(C) receptor agonist binding pocket. Constructing a complete model. *J. Biol. Chem.* **2005**, *280*, 1535−1542.

(23) Harrison, N. J.; Lummis, S. C. Molecular modeling of the GABA-(C) receptor ligand-binding domain. *J. Mol. Model. [Electronic Publication]* **2006**, *12*, 317−324.

(24) Frølund, B.; Ebert, B.; Kristiansen, U.; Liljefors, T.; Krogsgaard-Larsen, P. $GABA_A$ receptor ligands and their therapeutic potentials. *Curr. Med. Chem.* **2002**, *2*, 817−832.

(25) Frølund, B.; Jørgensen, A. T.; Tagmose, L.; Stensbøl, T. B.; Vestergaard, H. T.; Engblom, C.; Kristiansen, U.; Sanchez, C.; Krogsgaard-Larsen, P.; Liljefors, T. A novel class of potent 4-arylalkyl substituted 3-isoxazolol $GABA_A$ antagonists: synthesis, pharmacology and molecular modeling. *J. Med. Chem.* **2002**, *45*, 2454−2468.

(26) Crittenden, D. L. A quantitative structure−activity relationship investigation into agonist binding at $GABA_C$ receptors. *J. Mol. Struct.: THEOCHEM* **2005**, 81−89.

(27) Krehan, D.; Frølund, B.; Krogsgaard-Larsen, P.; Kehler, J.; Johnston, G. A.; Chebib, M. Phosphinic, phosphonic and seleninic acid bioisosteres of isonipecotic acid as novel and selective GABA(C) receptor antagonists. *Neurochem. Int.* **2003**, *42*, 561−565.

(28) Krehan, D.; Frølund, B.; Ebert, B.; Nielsen, B.; Krogsgaard-Larsen, P.; Johnston, G. A.; Chebib, M. Aza-THIP and related analogues of THIP as GABA C antagonists. *Bioorg. Med. Chem.* **2003**, *11*, 4891−4896.

(29) Johnston, G. A.; Curtis, D. R.; Beart, P. M.; Game, C. J.; McCulloch, R. M.; Twitchin, B. Cis- and trans-4-aminocrotonic acid as GABA analogues of restricted conformation. *J. Neurochem.* **1975**, *24*, 157−160.

(30) Chebib, M.; Johnston, G. A. Stimulation of [^{3}H]GABA and beta-[^{3}H]alanine release from rat brain slices by *cis*-4-aminocrotonic acid. *J. Neurochem.* **1997**, *68*, 786−794.

(31) Duke, R. K.; Chebib, M.; Balcar, V. J.; Allan, R. D.; Mewett, K. N.; Johnston, G. A. (+)- and (−)-*cis*-2-aminomethylcyclopropanecarboxylic acids show opposite pharmacology at recombinant rho(1) and rho(2) GABA(C) receptors. *J. Neurochem.* **2000**, *75*, 2602−2610.

(32) Murata, Y.; Woodward, R. M.; Miledi, R.; Overman, L. E. The first selective antagonist for a GABAC receptor. *Bioorg. Med. Chem. Lett.* **1996**, *6*, 2073−2076.

(33) Carver, D. S.; Lindell, S. D.; Saville-Stones, E. A. Polyfunctionalisation of imidazole via sequential imidazolyl anion formation. *Tetrahedron* **1997**, *53*, 14481−14496.

(34) Rosen, T.; Nagel, A. A.; Rizzi, J. P.; Ives, J. L.; Daffeh, J. B.; Ganong, A. H.; Guarino, K.; Heym, J.; McLean, S.; Nowakowski, J. T.; et al. Thiazole as a carbonyl bioisostere. A novel class of highly potent and selective 5-HT3 receptor antagonists. *J. Med. Chem.* **1990**, *33*, 2715−2720.

(35) Chadwick, D. J.; Ngochindo, R. I. 2,5-Dilithiation of N-protected imidazoles. Syntheses of 2,5-disubstituted derivatives of 1-methoxymethyl-, 1-triphenylmethyl-, and 1-(*N*,*N*-dimethylsulphonamide)-imidazole. *J. Chem. Soc., Perkin. Trans. 1* **1984**, 481−486.

(36) Widler, L.; Jaeggi, K. A.; Glatt, M.; Muller, K.; Bachmann, R.; Bisping, M.; Born, A. R.; Cortesi, R.; Guiglia, G.; Jeker, H.; Klein, R.; Ramseier, U.; Schmid, J.; Schreiber, G.; Seltenmeyer, Y.; Green, J. R. Highly potent geminal bisphosphonates. From pamidronate disodium (Aredia) to zoledronic acid (Zometa). *J. Med. Chem.* **2002**, *45*, 3721−3738.

(37) Durant, G. J.; Emmett, J. C.; Ganellin, C. R.; Roe, A. M.; Slater, R. A. Potential histamine H2-receptor antagonists. 3. Methylhistamines. *J. Med. Chem.* **1976**, *19*, 923−928.

(38) Stensbøl, T. B.; Uhlmann, P.; Morel, S.; Eriksen, B. L.; Felding, J.; Kromann, H.; Hermit, M. B.; Greenwood, J. R.; Brauner-Osborne, H.; Madsen, U.; Junager, F.; Krogsgaard-Larsen, P.; Begtrup, M.; Vedsø, P. Novel 1-hydroxyazole bioisosteres of glutamic acid. Synthesis, protolytic properties, and pharmacology. *J. Med. Chem.* **2002**, *45*, 19−31.

(39) Frølund, B.; Tagmose, L.; Liljefors, T.; Stensbøl, T. B.; Engblom, C.; Kristiansen, U.; Krogsgaard-Larsen, P. A novel class of potent 3-isoxazolol $GABA_A$ antagonists: design, synthesis, and pharmacology. *J. Med. Chem.* **2000**, *43*, 4930−4933.

(40) Frølund, B.; Jensen, L. S.; Guandalini, L.; Canillo, C.; Vestergaard, H. T.; Kristiansen, U.; Nielsen, B.; Stensbøl, T. B.; Madsen, C.; Krogsgaard-Larsen, P.; Liljefors, T. Potent 4-aryl- or 4-arylalkyl-substituted 3-isoxazolol GABA(A) antagonists: synthesis, pharmacology, and molecular modeling. *J. Med. Chem.* **2005**, *48*, 427−439.

(41) Hartvig, L.; Lukensmejer, B.; Liljefors, T.; Dekermendjian, K. Two conserved arginines in the extracellular N-terminal domain of the GABA(A) receptor alpha(5) subunit are crucial for receptor function. *J. Neurochem.* **2000**, *75*, 1746−1753.

(42) Boileau, A. J.; Evers, A. R.; Davis, A. F.; Czajkowski, C. Mapping the agonist binding site of the GABAA receptor: evidence for a beta-strand. *J. Neurosci.* **1999**, *19*, 4847−4854.

(43) Harrison, N. J.; Lummis, S. C. Locating the carboxylate group of GABA in the homomeric rho GABA(A) receptor ligand-binding pocket. *J. Biol. Chem.* **2006**, *281*, 24455−24461.

(44) Westh-Hansen, S. E.; Witt, M. R.; Dekermendjian, K.; Liljefors, T.; Rasmussen, P. B.; Nielsen, M. Arginine residue 120 of the human $GABA_A$ receptor α_1 subunit is essential for GABA binding and chloride ion current gating. *NeuroReport* **1999**, *10*, 2417−2421.

(45) Gallivan, J. P.; Dougherty, D. A. Cation−pi interactions in structural biology. *Proc. Natl. Acad. Sci. U.S.A.* **1999**, *96*, 9459−9464.

(46) Amin, J.; Weiss, D. S. $GABA_A$ receptor needs two homologous domains of the β-subunit for activation by GABA but not by pentobarbital. *Nature* **1993**, *366*, 565−569.

(47) Celie, P. H.; van Rossum-Fikkert, S. E.; van Dijk, W. J.; Brejc, K.; Smit, A. B.; Sixma, T. K. Nicotine and carbamylcholine binding to nicotinic acetylcholine receptors as studied in AChBP crystal structures. *Neuron* **2004**, *41*, 907−914.
(48) Lummis, S. C.; L., B. D.; Harrison, N. J.; Lester, H. A.; Dougherty, D. A. A cation−pi binding interaction with a tyrosine in the binding site of the GABAC receptor. *Chem. Biol.* **2005**, *12*, 993−997.
(49) Padgett, C. L.; Hanek, A. P.; Lester, H. A.; Dougherty, D. A.; Lummis, S. C. Unnatural amino acid mutagenesis of the GABA(A) receptor binding site residues reveals a novel cation−pi interaction between GABA and beta 2Tyr97. *J. Neurosci.* **2007**, *27*, 886−892.
(50) Wagner, D. A.; Czajkowski, C.; Jones, M. V. An arginine involved in GABA binding and unbinding but not gating of the GABA(A) receptor. *J. Neurosci.* **2004**, *24*, 2733−2741.
(51) Kloda, J. H.; Czajkowski, C. Agonist-, antagonist-, and benzodiazepine-induced structural changes in the alpha1 Met113-Leu132 region of the GABAA receptor. *Mol. Pharmacol.* **2007**, *71*, 483−493.
(52) Amin, J.; Weiss, D. S. Homomeric rho 1 GABA channels: activation properties and domains. *Recept. Channels* **1994**, *2*, 227−236.
(53) Allinger, N. L.; Yuh, Y. H.; Lii, J.-H. Molecular mechanics. The MM3 force field for hydrocarbons. 1. *J. Am. Chem. Soc.* **1989**, *111*, 8551−8566.
(54) Frølund, B.; Jensen, L. S.; Storustovu, S. I.; Stensbøl, T. B.; Ebert, B.; Kehler, J.; Krogsgaard-Larsen, P.; Liljefors, T. 4-Aryl-5-(4-piperidyl)-3-isoxazolol GABAA antagonists: synthesis, pharmacology, and structure−activity relationships. *J. Med. Chem.* **2007**, *50*, 1988−1992.
(55) Chang, Y.; Weiss, D. S. Channel opening locks agonist onto the GABAC receptor. *Nat. Neurosci.* **1999**, *2*, 219−225.
(56) Tunnicliff, G. Pharmacology and function of imidazole 4-acetic acid in brain. *Gen. Pharmacol.* **1998**, *31*, 503−509.
(57) Bouchet, M. J.; Rendon, A.; Wermuth, C. G.; Goeldner, M.; Hirth, C. Aryl diazo compounds and diazonium salts as potential irreversible probes of the gamma-aminobutyric acid receptor. *J. Med. Chem.* **1987**, *30*, 2222−2227.
(58) Orain, D.; Mattes, H. Synthesis of imidazole phosphinic acids as I4AA analogues. *Tetrahedron Lett.* **2006**, *47*, 1253−1255.
(59) Krzywkowski, K.; Jensen, A. A.; Connolly, C. N.; Bräuner-Osborne, H. Naturally occurring variations in the human 5-HT_{3A} gene profoundly impact 5-HT_3 receptor function and expression. *Pharmacogenenet. Genomics* **2007**, *17*, 255−266.
(60) Jensen, A. A.; Mikkelsen, I.; Frølund, B.; Brauner-Osborne, H.; Falch, E.; Krogsgaard-Larsen, P. Carbamoylcholine homologs: novel and potent agonists at neuronal nicotinic acetylcholine receptors. *Mol. Pharmacol.* **2003**, *64*, 865−875.
(61) Jensen, A. A.; Kristiansen, U. Functional characterisation of the human alpha1 glycine receptor in a fluorescence-based membrane potential assay. *Biochem. Pharmacol.* **2004**, *67*, 1789−1799.
(62) Chang, Y.; Covey, D. F.; Weiss, D. S. Correlation of the apparent affinities and efficacies of gamma-aminobutyric acid(C) receptor agonists. *Mol. Pharmacol.* **2000**, *58*, 1375−1380.
(63) Carland, J. E.; Moore, A. M.; Hanrahan, J. R.; Mewett, K. N.; Duke, R. K.; Johnston, G. A.; Chebib, M. Mutations of the 2′ proline in the M2 domain of the human GABAC rho1 subunit alter agonist responses. *Neuropharmacology* **2004**, *46*, 770−781.
(64) Chebib, M.; Mewett, K. N.; Johnston, G. A. GABA(C) receptor antagonists differentiate between human rho1 and rho2 receptors expressed in Xenopus oocytes. *Eur. J. Pharmacol.* **1998**, *357*, 227−234.
(65) Connor, D. S.; Klein, G. W.; Taylor, G. N.; Boeckmann, R. K., Jr.; Medwid, J. B. Benzyl chloromethyl ether. *Org. Synth., Collect. Vol.* **1988**, *6*, 101−103.
(66) Pedersen, D. S.; Rosenbohm, C. Dry column vacuum chromatography. *Synthesis* **2001**, 2431−2434.
(67) Gottlieb, H. E.; Kotlyar, V.; Nudelman, A. NMR chemical shifts of common laboratory solvents as trace impurities. *J. Org. Chem.* **1997**, *62*, 7512−7515.
(68) Reiter, L. A. Synthesis of 4(5)-acyl-, 1-substituted 5-acyl, and 1-substituted 4-acyl-1*h*-imidazoles from 4-aminoisoxazoles. *J. Org. Chem.* **1987**, 2714−2726.
(69) Jensen, A. A. Functional characterisation of human glycine receptors in a fluorescence-based high throughput screening assay. *Eur. J. Pharmacol.* **2005**, *521*, 39−42.
(70) Cheng, Y.; Prusoff, W. H. Relationship between the inhibition constant (Ki) and the concentration of inhibitor, which causes 50 per cent inhibition (I50) of an enzymatic reaction. *Biochem. Pharmacol.* **1973**, *22*, 3099−3108.
(71) Hamill, O. P.; Marty, A.; Neher, E.; Sakmann, B.; Sigworth, F. J. Improved patch-clamp techniques for high resolution current recording from cells and cell-free membranes. *Pfluegers Arch.* **1981**, *391*, 85−100.
(72) Frølund, B.; Kristiansen, U.; Brehm, L.; Hansen, A. B.; Krogsgaard-Larsen, P.; Falch, E. Partial GABAA receptor agonists. Synthesis and in vitro pharmacology of a series of nonannulated analogs of 4,5,6,7-tetrahydroisoxazolo[5,4-*c*]pyridin-3-ol. *J. Med. Chem.* **1995**, *38*, 3287−3296.
(73) Ebert, B.; Mortensen, M.; Thompson, S. A.; Kehler, J.; Wafford, K. A.; Krogsgaard-Larsen, P. Bioisosteric determinants for subtype selectivity of ligands for heteromeric GABA(A) receptors. *Bioorg. Med. Chem. Lett.* **2001**, *11*, 1573−1577.
(74) Ebert, B.; Frølund, B.; Diemer, N. H.; Krogsgaard-Larsen, P. Equilibrium binding characteristics of [^{3}H]thiomuscimol. *Neurochem. Int.* **1999**, *34*, 427−434.
(75) Ebert, B.; Wafford, K. A.; Whiting, P. J.; Krogsgaard-Larsen, P.; Kemp, J. A. Molecular pharmacology of gamma-aminobutyric acid type A receptor agonists and partial agonists in oocytes injected with different alpha, beta, and gamma receptor subunit combinations. *Mol. Pharmacol.* **1994**, *46*, 957−963.
(76) Chebib, M.; Vandenberg, R. J.; Froestl, W.; Johnston, G. A. Unsaturated phosphinic analogues of gamma-aminobutyric acid as GABA(C) receptor antagonists. *Eur. J. Pharmacol.* **1997**, *329*, 223−229.

JM070447J